Study on the assessment of hepatic congestion and fibrosis in dogs with cardiac disease using Shear Wave Elastography

（犬の心疾患における剪断波エラストグラフィを用いた肝うっ血および肝線維化の評価に関する研究）

Shiohara Nozomi

Contents

Abbreviations

2D-SWE; two-dimensional shear wave elastography
ACE; angiotensin converting enzyme
ALP; alkaline phosphatase
ALT; alanine aminotransferase
ASD; atrial septal defect
AUC; area under the curve
Cl; confidence interval
CVC; caudal vena cava
CVP; central venous pressure
DS; dispersion slope
LD; long diameter
LVOT-VTI; velocity time integral of left ventricular outflow tract
LA/Ao; left atrial to aortic root ratio
MMVD; myxomatous mitral valve disease
PDA; patent ductus arteriosus
PH; pulmonary hypertension
PS; pulmonic stenosis
RAA; right atrial area
RHF; right-sided heart failure
ROC; receiver-operating characteristic
ROI; region of interest
SD; short diameter
SWS; shear wave speed
T-Bill; total bilirubin
TRV; tricuspid regurgitant velocity
TVD; tricuspid valve dysplasia
VSD; ventricular septal defect

General Introduction

Heart failure represents the terminal stage of various cardiac diseases, including valvular heart disease, cardiomyopathy, and pulmonary hypertension. Once compensatory mechanisms are exhausted, systemic congestion and reduced cardiac output become the predominant pathophysiological features, predisposing patients to multi-organ dysfunction. Among the organs affected, the liver is particularly susceptible to the hemodynamic alterations associated with right-sided heart failure (RHF).

In RHF, increased central venous pressure (CVP) leads to passive hepatic congestion, resulting in dilation of hepatic veins, capillaries, and sinusoids, as well as compression of intrahepatic bile ducts. These changes cause hepatocellular atrophy and necrosis, and persistent congestion promotes chronic injury that may ultimately progress to hepatic fibrosis[1-6]. In human patients with heart failure, hepatic congestion has been identified as an important prognostic factor[7]. Moreover, reduced cardiac output can impair systemic and hepatic perfusion, producing centrilobular necrosis classically described as “hypoxic hepatitis” or “hypoxic liver injury.”[3-5, 8] Such hypoxic and congestive insults may synergistically accelerate hepatic fibrosis[9-11]. Thus, the liver is highly particularly susceptible to the hemodynamic burden of heart failure[1,3,4], underscoring the importance of accurate assessment of hepatic congestion and dysfunction in both human and veterinary patients.

The current gold standard for assessing systemic congestion involves direct measurement of CVP or right atrial pressure (RAP) via central venous or right heart catheterization. These hemodynamic indices are closely associated with prognosis in human heart failure[12]. However, in veterinary medicine, catheterization is an invasive procedure requiring general anesthesia and carries potential risks such as infection, hemorrhage, thrombosis, and valvular trauma[13-16]. Likewise, liver biopsy—the diagnostic gold standard for hepatic fibrosis and congestion—is invasive, associated with serious complications[17-18], and prone to sampling error due to heterogeneous distribution of lesions[19]. Accordingly, there is a substantial need for reliable, quantitative, and non-invasive methods to evaluate hepatic congestion.

In both canine and human patients, the caudal vena cava (CVC in dogs) and inferior vena cava (IVC in humans) are compliant vessels that dynamically change in diameter in response to fluctuations in CVP. Several studies have demonstrated that the diameters of the CVC and IVC correlate with CVP[20-22]. Consequently, ultrasonographic measurement of CVC and IVC diameters has been widely employed as a non-invasive surrogate marker of venous congestion. In particular, the ratio of the short diameter (SD) to the long diameter (LD) of the CVC (CVC SD/LD ratio) has shown good diagnostic accuracy for RHF[23]. However, because of their high compliance, the diameters of these veins are strongly influenced by respiratory variation. In human clinical settings, IVC respiratory variation can be standardized using a sniff maneuver. In veterinary medicine, however, such standardization is not possible because respiratory patterns cannot be uniformly controlled in animal patients. This respiratory dependency contributes to considerable interrater and intrapatient variability, limiting the reliability of these indices[24, 25]. These limitations highlight the need for more objective and quantitative imaging biomarkers of organ congestion.

Two-dimensional shear wave elastography (2D-SWE) is an advanced ultrasonographic technique that enables quantitative assessment of tissue mechanical properties by generating shear waves through acoustic radiation force and measuring their propagation velocity. The primary parameter obtained by 2D-SWE is shear wave speed (SWS), which reflects tissue viscoelasticity; higher SWS values indicate increased tissue stiffness[26-31]. In addition, a novel parameter called dispersion slope (DS) has been developed to evaluate tissue viscosity independently of elasticity. DS quantifies the frequency dispersion phenomenon—variation of SWS with the frequency of acoustic pulses—and higher DS values indicate greater tissue viscosity[32-35]. Increased tissue elasticity is typically associated with fibrosis, whereas increased viscosity is associated with inflammatory and congestive changes.

Previous experimental studies have demonstrated that congestion leads to increased viscoelasticity in hepatic tissues, as measured by 2D-SWE. In animal models, hepatic congestion induced by IVC clamping in pigs resulted in elevated SWS values[36,37]. Furthermore, our laboratory has reported a strong correlation between hepatic SWS measured by 2D-SWE and RAP in a canine model of volume overload–

induced liver congestion[38]. These findings suggest that 2D-SWE may serve as a promising tool for non-invasive assessment of hepatic congestion. In human patients with heart failure, both SWS and DS have been associated with disease severity and prognosis, further underscoring the clinical relevance of these parameters[39-42].

Despite these encouraging results, research on the application of 2D-SWE to naturally occurring canine heart disease remains limited, and its clinical significance is not fully established. Furthermore, since DS is a novel parameter, its potential utility as a biomarker for hepatic congestion or fibrosis in veterinary medicine remains unclear. Therefore, this study aimed to evaluate hepatic congestion and fibrosis in dogs with cardiac disease using 2D-SWE and to investigate the diagnostic value of both SWS and DS. This study aimed to characterize how SWS and DS change in dogs with heart disease, identify the factors associated with these variations, and evaluate their clinical utility.

Chapter 1

Evaluation of the utility of Two-Dimensional Shear Wave Elastography in assessing hepatic congestion induced by volume loading in dogs

1. Introduction

In veterinary medicine, the evaluation of hepatic congestion has mainly relied on indirect indicators such as liver enzyme activity, radiographic findings, or ultrasonographic features including hepatomegaly and dilation of the CVC and hepatic veins. However, these qualitative findings are influenced by hemodynamic and respiratory variations and lack quantitative accuracy[24, 25]. Thus, a reliable, non-invasive, and quantitative method for assessing hepatic congestion in dogs remains an unmet clinical need.

Previous study has demonstrated a strong correlation between hepatic SWS and RAP in a canine model of hepatic congestion induced by volume overload, suggesting that SWS may be a useful indicator for evaluating hepatic congestion[38]. However, SWS is also strongly influenced by hepatic fibrosis[26-31]. In clinical cases of cardiac disease, it is often difficult to determine whether an increase in SWS is due to reversible congestion or irreversible fibrosis. To overcome this limitation, a novel ultrasound parameter known as DS has been developed, which reflects tissue viscosity independently of elasticity[32-35]. Because DS is less affected by fibrosis and more closely related to congestion and inflammation, it may provide a more specific assessment of hepatic congestion than SWS. Nevertheless, the utility of DS for evaluating hepatic congestion has not yet been clarified in the veterinary field.

Therefore, this study aimed to evaluate the diagnostic utility of 2D-SWE, including both SWS and DS, in assessing hepatic congestion induced by volume overload in dogs. By performing 2D-SWE before and after blood transfusion in anemic dogs, we sought to determine whether these parameters could reflect hemodynamic changes associated with systemic congestion.

2. Materials and methods

2.1 Animals

Dogs that presented to Hokkaido university veterinary teaching hospital during April 2020 and December 2023 and received blood transfusions for anemia were prospectively included in the study. Data on age, sex, body weight, breed, and the type of transfusion product administered were recorded for all dogs. Each dog underwent physical examination, complete blood count, serum biochemical analysis, and abdominal ultrasonography. We excluded dogs with evident liver abnormalities, such as masses, changes in size or echogenicity detected on ultrasound examination; cases with significant alanine transaminase (ALT) elevations (>5 times the upper limit of normal, ≥390 U/L), hyperbilirubinemia; those receiving corticosteroids such as prednisolone; and cases with a history of neoplastic disease. All animal experiments were approved by Hokkaido University Veterinary Teaching Hospital (HUVTH-CR 21-01). Informed owner's consent was obtained in all cases.

2.2 Blood transfusion

The decision to transfuse was made by the respective treating veterinarian based on clinical and hematological variables and the severity of anemia. All patients received pre-transfusion medications consisting of famotidine (1 mg/kg subcutaneously) and diphenhydramine (2 mg/kg subcutaneously). The transfusion was initiated at a slow rate (0.5–1.0 mL/kg/h) for the first 30 min, after which the rate was gradually increased. The transfusion was completed within 4 h of initiation. During transfusion, heart rate, respiratory rate, rectal temperature, and physical appearance were monitored and recorded at least every 30 min using a standard transfusion monitoring protocol.

2.3 Measurement of 2D-SWE

Ultrasound imaging was performed using an ultrasound scanner (Aplio i800; Canon Medical Systems) with a convex probe (i8CX1, 1.8–6.2 MHz). 2D-SWE was conducted on the right lobe of the liver before and after transfusion, following human elastography guidelines and previously established protocols for dogs[31, 43, 44]. The right

lobe of the liver is deemed more appropriate for 2D-SWE measurements, as the left lobe is more prone to interference from adjacent organs, including the heart, lungs, and stomach[45, 46]. When performing 2D-SWE of the liver, the dogs were positioned in left lateral recumbency, the ultrasound probe was placed parallel to and within the intercostal space, and sufficient gel was applied to minimize rib shadowing. Hepatic images of the right lobe parenchyma were acquired using the intercostal approach under visual control in B-mode. To minimize the effect of respiratory motion, measurements were taken at the end-expiratory phase, and both SWS and DS were recorded. 2D-SWE measurements were performed immediately before the transfusion began and immediately after it ended.

The display mode can be switched post-data acquisition to one of four modes: speed, elasticity, propagation, or dispersion. In the speed mode, SWS is displayed as a color map (range, 0.5–6.5 m/s); in the elasticity mode, Young's modulus is mapped (range, 0–120 kPa); and in the dispersion mode, DS is mapped (range, 0–70 (m/s)/kHz). The SWS, Young's modulus, and DS values are visualized as color gradations, with blue, green, yellow, and red corresponding to increasing tissue stiffness. Areas in the color map that lack color-coding indicate the absence of shear waves (Figure 1). The propagation mode visually represents propagating shear waves within tissue as contour lines. Parallel contour lines indicate high reliability; thus, the region of interest (ROI) was assessed using the speed and dispersion modes. The ROI diameter was standardized to 10 mm and positioned within the parenchyma of the right hepatic lobe to avoid areas that were not color-coded or regions containing large blood vessels (Figure 1). Ten measurements were taken for each dog, and the median SWS and DS values of were recorded as representative measurements. 2D-SWE was conducted by a single sonographer with seven years of experience in SWE, ensuring consistent imaging conditions throughout the study.

2.4 Evaluation of congestion

The CVC was evaluated before and after transfusion as an indicator of congestion. Based on a previous study[23], a probe was placed in a transverse position between the 10th to 12th right dorsolateral intercostal spaces to acquire the CVC measurements

(Figure 2-A). If the CVC was not clearly visible, or if interference from the lungs or kidneys was present, the probe was moved one intercostal space cranially or caudally. The liver was used as the acoustic window to ensure a clear image of the CVC. All measurements were obtained with the dogs lying motionless and breathing quietly. The shape of the CVC varies with the respiratory phase, reaching its minimum during inspiration and maximum during expiration. Based on previous studies, the LD and the short diameter (SD), which is perpendicular to the LD, of the CVC were measured when the CVC reached its minimum size during inspiration (Figure 2-B). These values were recorded before and after the transfusion, and the minimum ratio of SD to LD (CVC SD/LD) was calculated as an index of congestion. A previous study reported that the CVC SD/LD is significantly elevated in dogs with RHF compared to healthy dogs or dogs with heart disease without RHF, with a cutoff value of 0.665 proving useful for identifying RHF[23].

2.5 Statistical analysis

Statistical analyses were performed using commercially available statistical software (JMP Pro version 17.2.0; SAS Institute, Cary, North Carolina, USA). All continuous variables were assessed for normality using the Shapiro-Wilk test. Data that followed a normal distribution are presented as mean ± standard deviation, whereas non-normally distributed data are reported as median and interquartile range. Paired t-tests were used to compare changes in SWS, DS, and CVC SD/LD before and after transfusion. The relationships between SWS, DS, and CVC SD/LD were analyzed using Pearson's correlation coefficients. Differences were considered statistically significant when P values were <0.05.

Figure 1. Speed mode (A, B) and dispersion mode (C, D) images of 2D-SWE in the liver

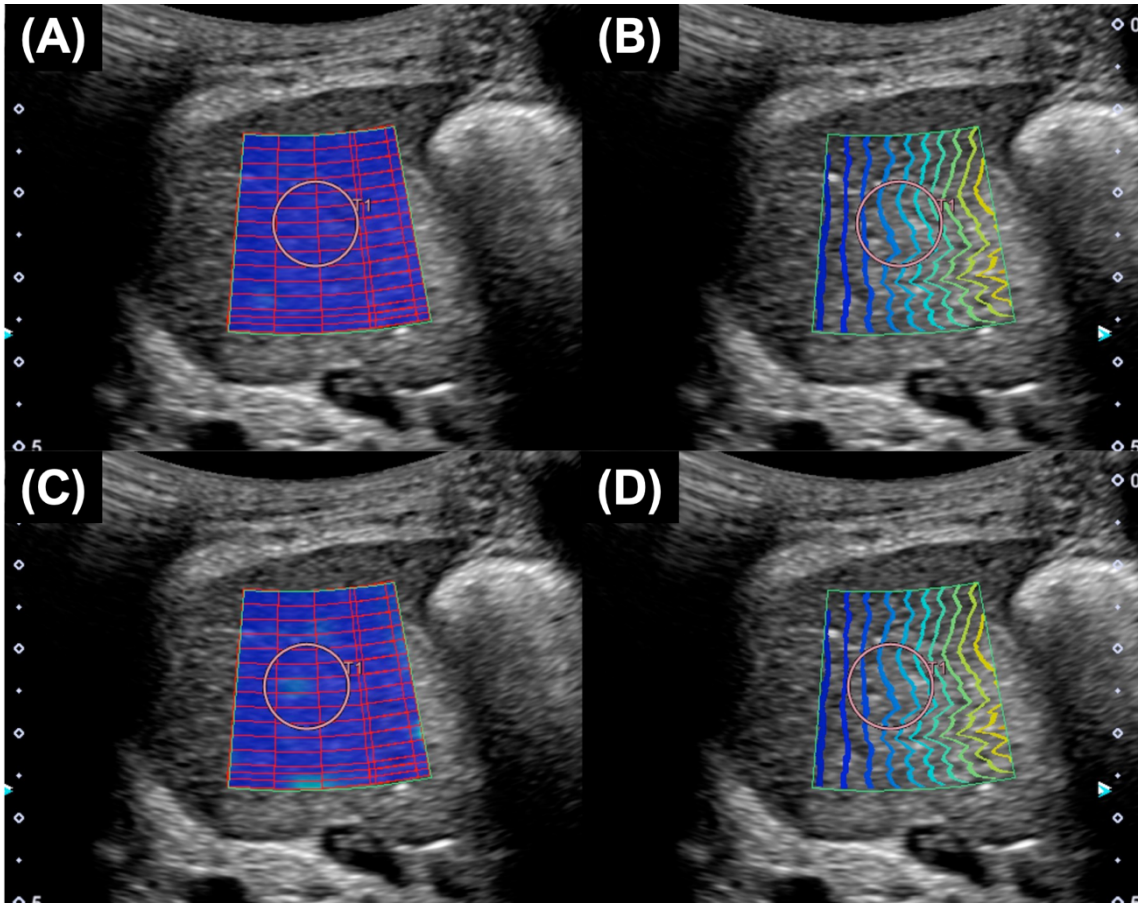

Speed mode displays the SWS map (A) and the propagation map (B), while dispersion mode shows the DS map (C) and the propagation map (D). Speed mode measures SWS in m/s, and dispersion mode measures DS in [(m/s)/kHz]. The circle in each map represents the region of interest (ROI: T1; 10 mm diameter).

Figure 2. Ultrasonographic measurement of the caudal vena cava (CVC) short-to-long diameter ratio (SD/LD)

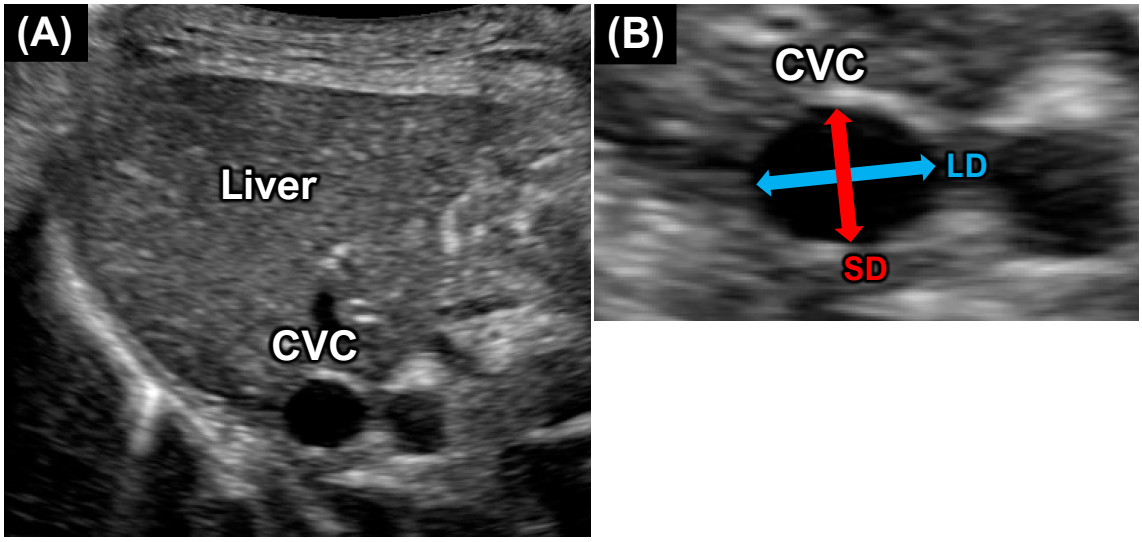

The CVC was visualized in a transverse plane at the level of the hepatic hilum (A). During inspiration, the maximal collapse of the CVC was identified, and the longest diameter (LD) along the vessel and the shortest diameter (SD) perpendicular to the LD were measured (B). The SD/LD ratio was calculated as an index of congestion.
CVC SD/LD: ratio of short diameter and long diameter of caudal vena cava

3. Results

3.1 Population characteristics

Of the dogs that received transfusions during the study period, 21 underwent 2D-SWE. One dog with an underlying lymphoma and three dogs with incomplete liver SWE data were excluded, leaving 17 dogs included in the study. Two of the 17 dogs received multiple transfusions, resulting in a total of 20 transfusions.

The cohort consisted of eight males and nine females, with a median age of 11.8 ± 4.1 years and a median body weight of 5.4 ± 1.9 kg. The breed distribution was as follows: six Miniature Dachshunds; two each of Chihuahua, American Cocker Spaniel, and Mixed breed; and one each of Toy Poodle, Pomeranian, Maltese, Cavalier King Charles Spaniel, and West Highland White Terrier. All animals were administered packed red blood cells at a dose of 20 mL/kg. No serious adverse reactions were observed during or after the transfusions.

3.2 Assessment of 2D-SWE and CVC Measurements

The SWS, DS, and CVC SD/LD results before and after transfusion are presented in Table 1. The liver SWS before and after transfusion was 1.33 ± 0.12 m/s and 1.75 ± 0.19 m/s, respectively, showing a significant increase post-transfusion (Figure 3-A). The liver DS values before and after transfusion were 12.05 ± 1.17 [(m/s)/Hz] and 16.85 ± 1.98 [(m/s)/Hz], respectively, also significantly higher after transfusion (Figure 3-B). The liver color map before transfusion was primarily dark blue for both SWS and DS, whereas after transfusion, it was light blue to green, indicating elevated values (Figure 4-A, B).

CVC SD/LD values before and after transfusion were 0.32 ± 0.11 and 0.72 ± 0.09, respectively, with a significant increase post-transfusion (Figure 3-C).

Correlations between the liver SWS, DS, and CVC SD/LD are shown in Figure 5. A moderate positive correlation was observed between the liver SWS and CVC SD/LD ($r = 0.781$, $P < 0.001$), whereas a strong positive correlation was observed between the liver DS and CVC SD/LD ($r = 0.900$, $P < 0.001$).

Table 1. Results of SWS, DS, and CVC SD/LD in the liver before and after transfusion

Parameter	Pre-Transfusion	Post-Transfusion	*P* value
Liver SWS (m/s)	1.33 ± 0.12	1.75 ± 0.19	< 0.001
Liver DS [(m/s)/Hz]	12.05 ± 1.17	16.85 ± 1.98	< 0.001
CVC SD/LD	0.32 ± 0.11	0.72 ± 0.09	< 0.001

CVC SD/LD: ratio of short diameter and long diameter of caudal vena cava; DS: dispersion slope; SWS: shear wave speed

Figure 3. Comparison of each variable before and after transfusion.

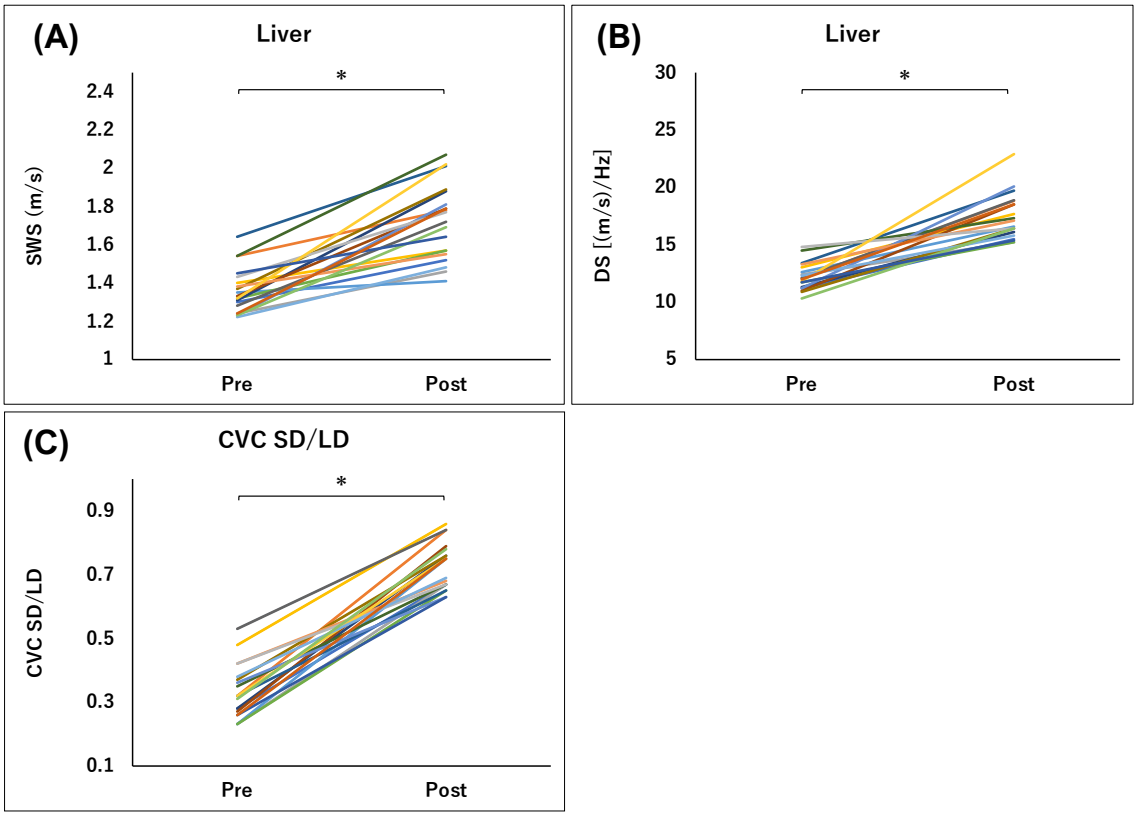

Each panel illustrates changes in hepatic SWS(A) and DS (B), CVC SD/LD (C) before and after transfusion. The asterisk (*) indicates a statistically significant difference with *P* values. CVC, caudal vena cava; LD, long diameter; SD, short diameter.

Figure 4. Color maps of SWS in the liver and before and after transfusion.

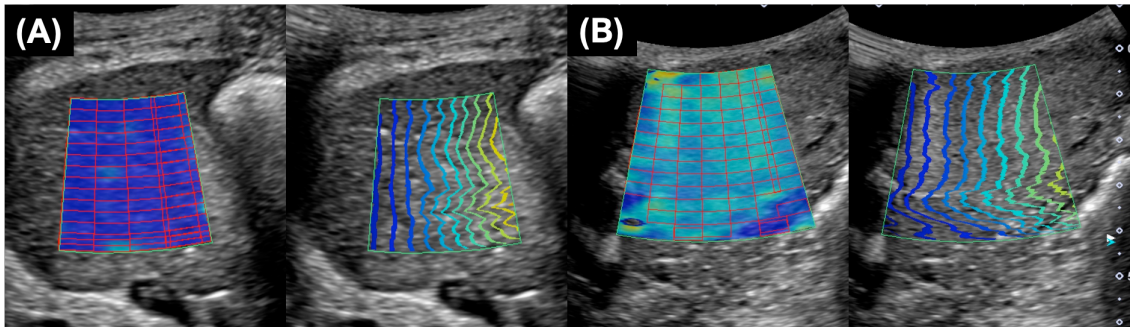

Before transfusion, the liver's color map was represented in dark blue (A), but after transfusion, it shifted to light blue to green (B), indicating an increase in SWS. SWS, shear wave speed.

Figure 5. Correlation between liver SWS, DS, and CVC SD/LD.

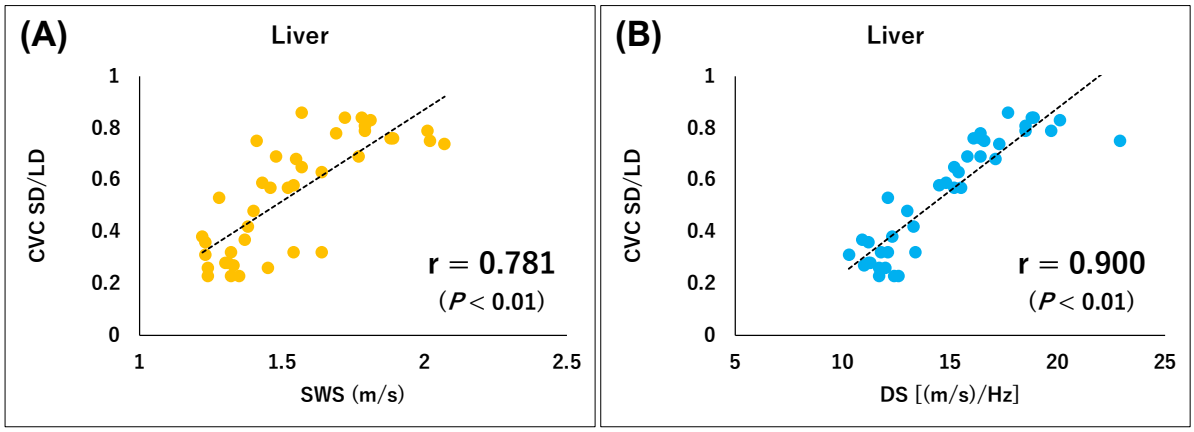

A moderate positive correlation was observed between liver SWS and CVC SD/LD (r = 0.781, $P < 0.001$). A strong positive correlation was found between liver DS and CVC SD/LD (r = 0.900, $P < 0.001$)

4. Discussion

In this study, 2D-SWE was used to assess the liver before and after transfusion to evaluate the efficacy of SWS and DS in detecting hepatic congestion. 2D-SWE measurements were conducted on the right hepatic lobe.

Congestion and CVC

In the medical field, ultrasonographic examination of the IVC is a routine and noninvasive method for estimating RAP and CVP, with various IVC parameters demonstrating utility[21,22,45-47]. Specifically, the ratio of the SD to the LD of the IVC (IVC SD/LD) correlates well with CVP and serves as a reliable indicator of congestion[47,48]. Although there are no veterinary studies comparing CVC SD/LD directly with CVP or RAP, CVC SD/LD has been reported to be significantly elevated in dogs with RHF compared to healthy dogs or dogs with heart disease without RHF, indicating its diagnostic potential for RHF[23]. The results of this study further support this finding, demonstrating that CVC SD/LD significantly increases after blood transfusion, suggesting its potential utility in assessing clinical congestion in veterinary practice.

SWS for liver congestion

This study found a significant increase in the liver SWS after transfusion. Tissue stiffness is affected by both elasticity and viscosity. Elasticity is primarily increased by fibrosis, making SWS a valuable indicator of fibrosis in both the medical and veterinary fields[26-31]. Conversely, several studies in humans and dogs have indicated that viscous factors, such as inflammation and bile congestion related to extrahepatic bile duct obstruction, can elevate liver SWS[50-54]. This has led to growing interest in the utility of SWS as an indicator of tissue viscosity. Furthermore, experimental studies in pigs[36,37] and dogs[38] have demonstrated that hepatic congestion, as a viscous factor, elevated SWS. Experimental models in pigs[36,37], in which the IVC was clamped to induce hepatic congestion, showed a marked increase in liver SWS, correlating perfectly with CVP ($r = 1.00$). Furthermore, when the IVC was unclamped, the SWS decreased to

baseline levels, similar to those observed before clamping. Histopathological examination revealed enlarged central veins and sinusoids within the hepatic lobes, along with hepatocyte edema—findings consistent with hepatic congestion. Similarly, canine models[38] subjected to intravenous volume overload showed a significant increase in liver SWS and strong correlation with RAP (r = 0.9729). The present study corroborates these findings by demonstrating a significant increase in liver SWS with volume loading, likely reflecting increased viscosity due to hepatic congestion. However, the correlation between the SWS and CVC SD/LD was moderate (r = 0.781). This might be attributed to a potential dissociation between the CVC SD/LD and CVP. While a positive correlation between the IVC SD/LD and CVP has been observed in human studies (r=0.75-0.849)[48,49], such data are lacking in veterinary literature. Additionally, because the CVC is sensitive to respiratory changes, a lower correlation with CVP is expected in dogs, where controlling breathing is more challenging than in humans. Studies on dogs have documented significant interrater variability between CVC measurements[24,25]. Therefore, the results of this study do not refute the correlation between SWS and CVP; rather, they suggest that SWS may have a stronger correlation with CVP than with the CVC variables.

DS for liver congestion

DS is a novel indicator in 2D-SWE that estimates tissue viscosity based on the frequency dependence of shear waves. Although DS has been reported to be elevated in conditions such as hepatitis and fatty liver[32-35, 55-57], its use for assessing congestion is less well documented. Studies on human cardiac patients have reported elevated liver DS levels with increasing severity of cardiac disease[40]. In this study, a moderate correlation (r = 0.45) was observed between liver DS and right atrial size; however, there was no significant correlation with RAP. Another study identified high liver DS as an independent prognostic factor in human patients with heart disease, although it found no substantial correlation between DS and congestion indices such as IVC diameter or RAP[39]. Additionally, a weak correlation (r = 0.177) was observed between DS and P4NP7S, a marker of liver fibrosis. These findings may be attributed to the fact that SWE and RAP measurements were conducted during the chronic phase of heart failure,

potentially missing the peak of elevated CVP during the acute phase. Furthermore, factors such as liver fibrosis and inflammation resulting from chronic congestion and heart failure may have confounded the results.

In our study, DS values were significantly elevated after transfusion, similar to SWS values. Given that SWE was performed immediately after the transfusion, secondary fibrosis was unlikely, indicating that the observed changes were attributable to increased viscosity due to congestion. DS demonstrated a stronger correlation with CVC SD/LD ($r = 0.900$) than with SWS ($r = 0.781$), suggesting that DS is a more reliable indicator of congestion. Future studies are needed to compare DS and SWS using direct CVP measurements to further validate the relative effectiveness of DS.

In this study, 2D-SWE measurements were taken only immediately after transfusion, and it was not possible to assess whether the elevated SWS and DS were temporary changes. However, previous studies in dogs and pigs have reported that the increase in SWS induced by volume loading is reversible and returns to baseline over time[36,37]. Therefore, the changes in SWS and DS observed in this study are likely reversible and are expected to improve with fluid redistribution.

The results of this study indicate that 2D-SWE, which measures both SWS and DS, can be a valuable noninvasive tool for evaluating liver congestion. However, in heart failure, the stiffness of these organs can be influenced by both congestion and fibrosis. Chronic congestion in patients with heart failure can lead to fibrosis of the liver,[1, 6, 58, 59], and chronic liver disease can contribute to hepatic fibrosis and dysfunction. Given that fibrosis is irreversible whereas congestion may improve with early treatment, it is crucial to differentiate between these conditions[60-62]. However, because both congestion and fibrosis increase tissue stiffness (viscoelasticity), distinguishing between them using the current viscoelasticity index (SWS) is challenging. DS, a newer index that specifically measures viscosity without being influenced by elasticity, can help differentiate between fibrosis and congestion. Combining SWS and DS may provide a more accurate assessment of liver conditions.

Further studies are needed to validate the effectiveness of 2D-SWE in distinguishing these conditions in patients with cardiac disease.

Clinical Implications and Practical Considerations

2D-SWE represents a promising non-invasive modality for the assessment of organ congestion. However, interpretation of SWS values requires caution, as elevations may also be observed in the presence of fibrosis. DS, which reflects tissue viscosity independently of elasticity, may help address this limitation. Nevertheless, increased DS values can also be influenced by other viscosity-related factors, such as inflammation, and these potential confounders should be taken into account in clinical interpretation.

Limitations

This study has several limitations. First, the sample size was limited, and the congestion induced by volume loading may not fully represent the pathophysiology of naturally occurring conditions. Second, CVP, the gold standard for measuring congestion, was not assessed, which may have affected the accuracy of the congestion evaluation. Third, histopathological examination was not performed, and other concurrent diseases that affect liver stiffness may have been present. Fourth, this study did not include cardiac function data (e.g., cardiac output and systemic vascular resistance), and the possibility that these factors may have confounded the 2D-SWE measurements cannot be excluded.

5. Summary

Heart failure, the terminal stage of various cardiac diseases, is frequently accompanied by hepatic congestion due to elevated central venous pressure. Hepatic congestion is an important pathophysiological condition closely associated with the prognosis of heart failure; however, a simple and quantitative method for evaluating its severity has not yet been established. Two-dimensional shear wave elastography (2D-SWE) is a noninvasive ultrasound technique that estimates tissue stiffness by measuring shear wave speed (SWS), an index of tissue viscoelasticity, and dispersion slope (DS), which reflects tissue viscosity alone. This study aimed to assess the utility of SWS and DS in evaluating hepatic congestion in dogs by performing 2D-SWE before and after blood transfusion. The ratio of the short to long diameter of the caudal vena cava (CVC SD/LD ratio) was used as an ultrasonographic index of systemic venous congestion. A total of 20 transfusions were administered to 17 dogs. After transfusion, both hepatic SWS and DS, as well as the CVC SD/LD ratio, increased significantly *(P* < 0.01). A moderate positive correlation was observed between the CVC SD/LD ratio and hepatic SWS (r = 0.781, *P* < 0.01), whereas a strong positive correlation was found between the CVC SD/LD ratio and hepatic DS (r = 0.900, *P* < 0.01). These findings suggest that 2D-SWE may serve as a valuable, noninvasive tool for assessing hepatic congestion in dogs, with DS potentially providing a more sensitive and reliable indicator of congestion than SWS.

Chapter 2

Assessment of hepatic Shear Wave Speed and Dispersion Slope using Two-Dimensional Shear Wave Elastography in dogs with heart disease

1. Introduction

Based on the findings of Chapter 1, both of SWS and DS was predominantly increased in hepatic congestion. In dogs with cardiac disease, chronic elevation of CVP resulting from RHF leads to hepatic congestion, which can progress to fibrosis with persistent or recurrent hemodynamic overload. Therefore, in clinical settings, both reversible congestion and irreversible fibrosis may coexist in varying proportions within the same liver, making it challenging to distinguish between these pathophysiological processes using conventional diagnostic modalities.

Ultrasonographic findings such as hepatomegaly and dilation of the CVC and hepatic veins are commonly used to evaluate hepatic congestion in dogs. However, these morphological changes are subjective and influenced by factors such as respiration, body condition, and imaging angle, resulting in considerable variability[24,25]. Similarly, biochemical parameters such as serum liver enzyme activities are nonspecific and may not accurately reflect the degree of hepatic structural change. Consequently, there remains a need for reliable, quantitative, and non-invasive indices that can detect hepatic congestion at an early, potentially reversible stage and differentiate it from established fibrosis.

2D-SWE enables quantitative assessment of hepatic viscoelastic properties through the measurement of SWS and DS. Given that SWS reflects elasticity and correlates with fibrosis, while DS reflects viscosity and correlates with congestion and inflammation, combined evaluation of these two parameters may allow for more detailed characterization of hepatic pathophysiology in dogs with heart disease[26-35]. Furthermore, since 2D-SWE can be performed repeatedly and non-invasively, it offers potential utility not only for initial diagnosis but also for longitudinal monitoring of treatment response and disease progression.

Therefore, this chapter aimed to measure and compare SWS and DS in the livers of dogs with naturally occurring heart disease, to clarify their clinical significance and to identify factors contributing to variation in these parameters.

2. Materials and methods

2.1 Animals

Client-owned dogs in which structural cardiac abnormalities were detected by echocardiographic examination were prospectively enrolled from cases presented to the Hokkaido University Veterinary Teaching Hospital between January 2021 and June 2025. Dogs were excluded if they had a history of primary liver disease; ultrasonographic evidence of hepatic parenchymal abnormalities (e.g., masses, parenchymal echogenic changes, irregular margins); marked increases in serum alanine aminotransferase (ALT > 5 × the upper reference limit, >390 U/L); hyperbilirubinemia (>0.5 mg/dL); severe hypoalbuminemia (<1.6 g/dL); or were receiving corticosteroids such as prednisolone. Dogs with neoplasia or portal vein thrombosis, which may cause effusion unrelated to heart disease, were also excluded based on abdominal ultrasonography.

For all cases, age, sex, body weight, breed, concurrent cardiovascular medications, and type of underlying structural heart disease (e.g., valvular disease, pulmonary hypertension [PH], congenital heart disease) were recorded. Abdominal ultrasonography was performed in all dogs to confirm the presence or absence of ascites. Dogs with ascites were classified as the RHF group, and those without ascites as the non-RHF group. If ascites could be sampled, peritoneal fluid analysis via paracentesis was performed to confirm transudative ascites. In cases where sampling was not possible, disappearance of ascites following treatment for heart failure was used to classify dogs into the RHF group. The study protocol was approved by the Institutional Animal Care and Use Committee of the Hokkaido University Veterinary Teaching Hospital (HUVTH-CR 21-01). Informed consent was obtained from all owners prior to enrollment.

2.2 Echocardiography

Echocardiography was performed by a single experienced veterinarian using either an Artida system (Toshiba Medical Systems, Tochigi, Japan; 4.4–6.2 MHz sector probe) or a Vivid E95 system (GE Healthcare, Chicago, IL, USA; 2.7–8.0 MHz sector

probe). Dogs were examined in right and left lateral recumbency without sedation, and a simultaneous lead II ECG was recorded.

B-mode and color doppler imaging were used to assess cardiac morphology, chamber enlargement, and abnormal blood flow (e.g., valvular regurgitation, shunt lesions). The diagnosis of pulmonary hypertension (PH) was based on the American College of Veterinary Internal Medicine guidelines[63], and cases with a high probability of PH were included and subclassified as Group 1 (pulmonary arterial hypertension due to congenital shunt), Group 2 (PH secondary to left heart disease), or PH of unknown origin.

As an index of left atrial size, the left atrial-to-aortic root diameter ratio (LA/Ao) was obtained in the right parasternal short-axis view immediately after aortic valve closure[64,65]. Stroke volume was estimated by measuring the left ventricular outflow tract velocity-time integral (LVOT-VTI) from an apical five-chamber view using pulsed doppler at the aortic valve annulus (Figure 8). Tricuspid regurgitation (TR) was assessed with color doppler, and maximum TR velocity (TRV) was obtained using continuous-wave doppler when present.

Echocardiographic examination of the right atrium was performed from the left apical 4-chamber view optimized for the right heart. Right atrial area (RAA) was measured by tracing right atrium at end-systole, excluding the area between the leaflets and annulus, following the right atrial endocardium, and excluding the caudal vena cava, cranial vena cava, and right atrial appendage. The RAA index[66] was calculated as RAA divided by body surface area as an indicator of right atrial enlargement (Figure 9). All measurements were performed offline by a single operator evaluating 3 cardiac cycles, and mean values were calculated.

2.3 Two-dimensional Shear Wave Elastography (2D-SWE)

Ultrasound imaging was performed using an Aplio i800 ultrasound system (Canon Medical Systems) with a convex probe (i8CX1, 1.8–6.2 MHz) same with Chapter 1 and 2. 2D-SWE was conducted on the right lobe of the liver following human elastography guidelines and previously established protocols for dogs[31, 43, 44]. When performing 2D-SWE of the liver, the dogs were positioned in left lateral recumbency, the ultrasound

probe was placed parallel to and within the intercostal space, and sufficient gel was applied to minimize rib shadowing. Hepatic images of the right lobe parenchyma were acquired using the intercostal approach under visual control in B-mode. To minimize the effect of respiratory motion, measurements were taken at the end-expiratory phase, and both SWS and DS were recorded. In the speed mode, SWS is displayed as a color map (range, 0.5–6.5 m/s) and in the dispersion mode, DS is mapped (range, 0–70 (m/s)/kHz). The SWS and DS values are visualized as color gradations, with blue, green, yellow, and red corresponding to increasing tissue stiffness. Areas in the color map that lack color-coding indicate the absence of shear waves (Figure 1). The propagation mode visually represents propagating shear waves within tissue as contour lines. Parallel contour lines indicate high reliability; thus, the region of interest (ROI) was assessed using the speed and dispersion modes. The ROI diameter was standardized to 10 mm and positioned within the parenchyma of the right hepatic lobe to avoid areas that were not color-coded or regions containing large blood vessels (Figure 1). Ten measurements were taken for each dog, and the median SWS and DS values were recorded as representative measurements. 2D-SWE was conducted by a single sonographer with seven years of experience in SWE, ensuring consistent imaging conditions throughout the study.

2.4 Assessment of Congestion

The caudal vena cava (CVC) was evaluated by abdominal ultrasound as an indicator of systemic venous congestion same with Chapter1. Following the protocol described in a previous study[23], the probe was positioned transversely between the 10th and 12th right dorsolateral intercostal spaces (Figure 2-A). When the CVC could not be clearly visualized, or when image quality was compromised by interference from the lungs or kidneys, the probe was adjusted one intercostal space cranially or caudally. The liver served as the acoustic window to optimize visualization of the CVC. All measurements were obtained with dogs in lateral recumbency, lying quietly and breathing spontaneously.

The morphology of the CVC varied with the respiratory cycle, reaching its minimum dimension during inspiration and its maximum during expiration. In

accordance with previous reports, the long diameter (LD) and short diameter (SD; measured perpendicular to the LD) were obtained at end-inspiration, when the CVC diameter was smallest (Figure 2-B). The minimum ratio of SD to LD (CVC SD/LD) was calculated as an index of venous congestion. A prior study demonstrated that the CVC SD/LD is significantly increased in dogs with RHF compared with both healthy dogs and dogs with cardiac disease without RHF, with a cutoff value of 0.665 providing diagnostic utility for RHF[23].

2.5 Statistical analysis

Data distribution was assessed using the Shapiro–Wilk test. Variables with normal distribution were expressed as mean ± standard deviation, whereas non-normally distributed variables were expressed as median (interquartile range). Statistical analyses were performed using commercial software (JMP Pro 17, SAS Institute Inc., Cary, NC, USA; EZR on R commander, Saitama Medical Center, Jichi Medical University, Saitama, Japan).

Differences between groups (RHF vs. non-RHF) were evaluated using the Wilcoxon rank-sum test. Variables showing significant differences were further analyzed by receiver operating characteristic (ROC) curve analysis, and the area under the curve (AUC) was calculated. AUC values were interpreted as follows: >0.9, strong correlation; 0.7–0.9, moderate correlation; 0.5–0.7, weak correlation; ≤0.5, no correlation[67]. Optimal cutoff values and their corresponding sensitivity and specificity were determined using the Youden index[68].

Spearman's rank correlation coefficients were calculated to examine associations among clinical variables. Multiple regression analysis was performed with SWS and DS as dependent variables, and LVOT-VTI, CVC SD/LD, TRV, and RAA index as explanatory variables. Stepwise variable selection was applied. For all statistical comparisons, differences were considered statistically significant when *P* values were <0.05.

Figure 8. Measurement of left ventricular outflow tract velocity–time integral (LVOT-VTI)

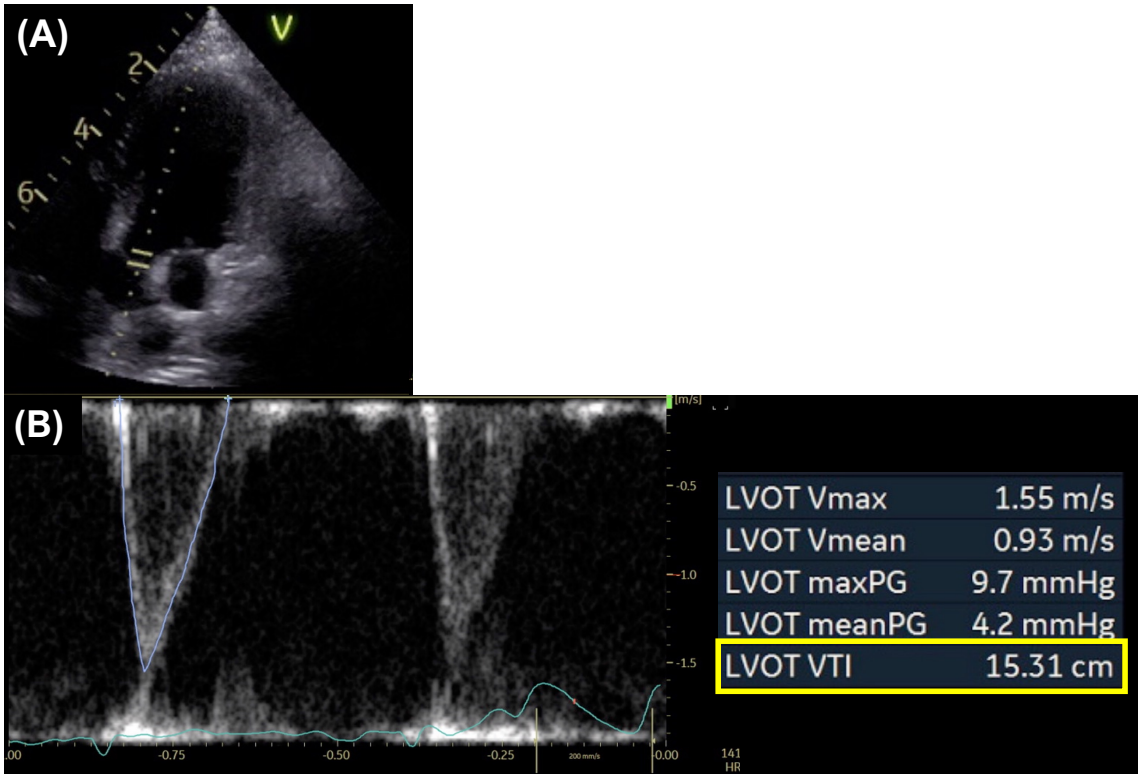

(A) From the left apical five-chamber view, the pulsed Doppler sample gate was positioned at the level of the aortic annulus in the left ventricular outflow tract. (B) The LVOT-VTI (15.31 cm) was measured by tracing the outer contour of the Doppler spectral envelope.

Figure 9. Measurement of right atrial area (RAA)

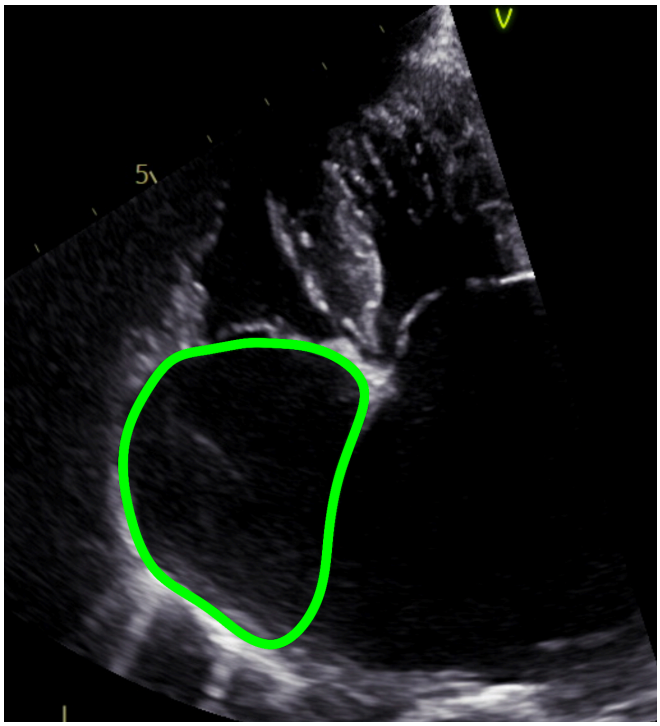

From an apical four-chamber view optimized for the right atrium, the endocardial border of the right atrium was traced at end-systole to obtain the RAA.

3. Results

3.1 Population characteristics

During the study period, 112 client-owned dogs that underwent echocardiography and were found to have structural cardiac abnormalities underwent 2D-SWE of the liver. Four dogs were excluded due to a history of chronic corticosteroid administration (n = 2) or concomitant neoplastic disease (n = 2), and eight additional dogs were excluded because of insufficient imaging or clinical data. The final study population comprised 100 dogs.

The non-RHF group included 73 dogs (20 Chihuahuas, 11 mixed breeds, 10 Toy Poodles, 6 Pomeranians, 3 Maltese, 3 Miniature Dachshunds, 3 Miniature Schnauzers, 3 Shih Tzus, 3 Boston Terriers, and 11 others), while the RHF group included 27 dogs (4 Chihuahuas, 4 mixed breeds, 3 French Bulldogs, 2 Toy Poodles, 2 Pomeranians, 2 Shiba Inus, 2 Boston Terriers, 2 Miniature Schnauzers, and 6 others). Signalment, serum biochemical test results, medication history, and diagnosed cardiac diseases are summarized in Table 5.

There were no significant differences between the non-RHF and RHF groups in terms of sex distribution, age, or body weight. Regarding cardiac medications, loop diuretic use was significantly higher in the RHF group ($P < 0.001$), whereas no differences were observed between the groups for other medications.

Regarding liver-related serum biochemical parameters, ALT ($P = 0.021$) and ALP ($P = 0.020$) were significantly higher in the RHF group, whereas total bilirubin did not differ significantly between the groups ($P = 0.323$).

The distribution of cardiac diseases in the non-RHF group was as follows: 48 cases of myxomatous mitral valve disease (MMVD) without PH, 8 cases of PH of unknown origin, 5 cases of atrial septal defect or ventricular septal defect (ASD/VSD), 4 cases of cardiomyopathy (dilated or hypertrophic), and 3 cases each of patent ductus arteriosus (PDA) or pulmonary artery stenosis (PS), with 2 cases of PH secondary to left heart disease (PH Group 2).

In the RHF group, the distribution was as follows: 10 cases of PH Group 2, 10 cases of PH of unknown origin, 4 cases of cardiac tamponade, and 1 case each of PH due to congenital heart disease (ASD, PH Group 1), pulmonary artery stenosis, and tricuspid valve dysplasia.

3.2 Ultrasonography and 2D-SWE parameters

Ultrasonographic findings, 2D-SWE measurements, and caudal vena cava (CVC) parameters for each group are summarized in Table 2. Compared to the non-RHF group, dogs in the RHF group had significantly lower LVOT-VTI ($P < 0.001$) and significantly higher TRV and RAA index (both $P < 0.001$). No significant difference was observed in LA/Ao between the groups ($P = 0.880$).

The median hepatic SWS was 1.31 m/s (interquartile range, 1.25–1.37) in the non-RHF group and 1.79 m/s (1.63–2.38) in the RHF group, with significantly higher values in the RHF group ($p < 0.001$). The median DS was 12.0 (11.0–13.5) in the non-RHF group and 16.4 (15.6–20.8) in the RHF group, also significantly higher in the RHF group ($P < 0.001$). Color maps of the liver in most non-RHF dogs were predominantly dark blue for both SWS and DS (Figure 10-A, B), whereas those in the RHF group were displayed as light blue to green to orange, reflecting elevated values (Figure 10-C, D).

The CVC SD/LD ratio was significantly higher in the RHF group compared to the non-RHF group, with median values of 0.44 (0.33–0.53) and 0.69 (0.61–0.76), respectively ($P < 0.001$).

3.3 Comparison of 2D-SWE Measurements with Other Parameters

Correlations between SWS, DS, and other clinical parameters are summarized in Table 6. A strong positive correlation was observed between SWS and DS ($r = 0.83$, $P < 0.001$). Both SWS and DS showed moderate positive correlations with CVC SD/LD, RAA index, and TRV, and a moderate negative correlation with LVOT-VTI.

3.4 Diagnostic performance of each parameter for detecting RHF

To evaluate the diagnostic performance of each parameter for identifying RHF, ROC curves and corresponding AUCs were calculated. As shown in Table 6, DS

demonstrated the highest diagnostic accuracy, followed by SWS, CVC SD/LD, RAA index, and LVOT-VTI.

3.5 Factors influencing the elevation of SWS and DS

Stepwise multiple regression analysis was performed to identify factors associated with SWS and DS, using parameters that showed significant differences between groups (ALT, ALP, LVOT-VTI, TRV, RAA index, and CVC SD/LD) as explanatory variables (Table 7). For SWS, the most strongly associated parameter was RAA index ($P < 0.0001$), followed by LVOT-VTI ($P = 0.0168$) and CVC SD/LD ($p = 0.0350$). For DS, CVC SD/LD was the most strongly associated parameter ($P < 0.0001$), followed by RAA index ($P = 0.0009$); no significant association was observed between DS and LVOT-VTI ($P = 0.167$).

Table 5. Signalment and clinical data of non-RHF and RHF dogs

	Non-RHF (n=73)	RHF (n=27)	*P* value
Age (years)	**11.2 (9.1–13.2)**	**12 (9.4–13.1)**	**0.296**
Sex (male/female)	**31/42**	**16/11**	**0.473**
Body weight (kg)	**4.0 (2.8-6.4)**	**5.6 (4.2-9.1)**	**0.160**
Meication			
ACE inhibitor	**15 (20.5%)**	**7 (25.9%)**	**0.291**
Pimobendan	**36 (49.3%)**	**15 (55.6%)**	**0.235**
Loop diuretics	**13 (17.8%)**	**18 (66.7%)**	**<0.001**
Spironolactone	**8 (11.0%)**	**4 (14.8%)**	**0.466**
Sildenafil	**3 (4.1%)**	**4 (14.8%)**	**0.071**
Liver enzyme			
ALT (IU/L)	**65 (42-103)**	**88 (62.2-142)**	**0.021**
ALP (U/L)	**99 (51.5-177.5)**	**150 (80.5-344.8)**	**0.020**
T-Bill (mg/dL)	**0.2 (0.1-0.2)**	**0.1 (0.1-0.2)**	**0.323**
Cardiac diseases			
MMVD	**48 (65.8%)**	**0**	**<0.001**
PH Group1	**0**	**1 (3.7%)**	**0.270**
PH Group2	**2 (2.7%)**	**10 (37.0%)**	**<0.001**
PH of unknown origin	**8 (11.0%)**	**10 (37.0%)**	**0.0045**
ASD/VSD	**5 (6.8%)**	**0**	**0.199**
Cardiomyopathy	**4 (5.5%)**	**0**	**0.278**
PDA	**3 (4.1%)**	**0**	**0.385**
PS	**3 (4.1%)**	**1 (3.7%)**	**0.706**
TVD	**0**	**1 (3.7%)**	**0.270**
Cardiac tamponade	**0**	**4 (14.8%)**	**0.0045**

ACE: angiotensin converting enzyme; ALP: alkaline phosphatase; ALT: alanine aminotransferase; ASD: atrial septal defect: MMVD: myxomatous mitral valve disease; PDA: patent ductus arteriosus; PH: pulmonary hypertension; PS: pulmonic stenosis; T-Bill: total bilirubin; TVD: tricuspid valve dysplasia; VSD: ventricular septal defect

Table 6. Echocardiographic, 2D-shear wave elastography, and CVC parameters in dogs of the non-RHF and RHF Groups

	Non-RHF	RHF	*P* value
LA/Ao	1.73 (1.43-2.29)	1.53 (1.41-3.00)	0.88
LVOT-VTI (m/s)	9.63 (8.18-11.82)	5.86 (5.01-6.68)	< 0.001
TRV (m/s)	3.13 (2.72-3.47)	4.14 (3.87-4.59)	< 0.001
RAA index	8.02 (6.38-10.98)	18.35 (13.63-21.08)	< 0.001
SWS (m/s)	1.31 (1.25-1.37)	1.79 (1.63-2.38)	< 0.001
DS [(m/s)/Hz]	12.0 (11.0-13.50)	16.40 (15.60-20.80)	< 0.001
CVC SD/LD	0.44 (0.33-0.53)	0.69 (0.61-0.76)	< 0.001

CVC SD/LD: ratio of short diameter and long diameter of caudal vena cava; DS: dispersion slope; LA/Ao: left atrial to aortic root ratio; LVOT-VTI: velocity time integral of left ventricular outflow tract; RAA index: right atrial area index; SWS: shear wave speed; TRV: tricuspid regurgitant velocity

Figure 10. Color maps of SWS and DS in dogs of the non-RHF and RHF Groups

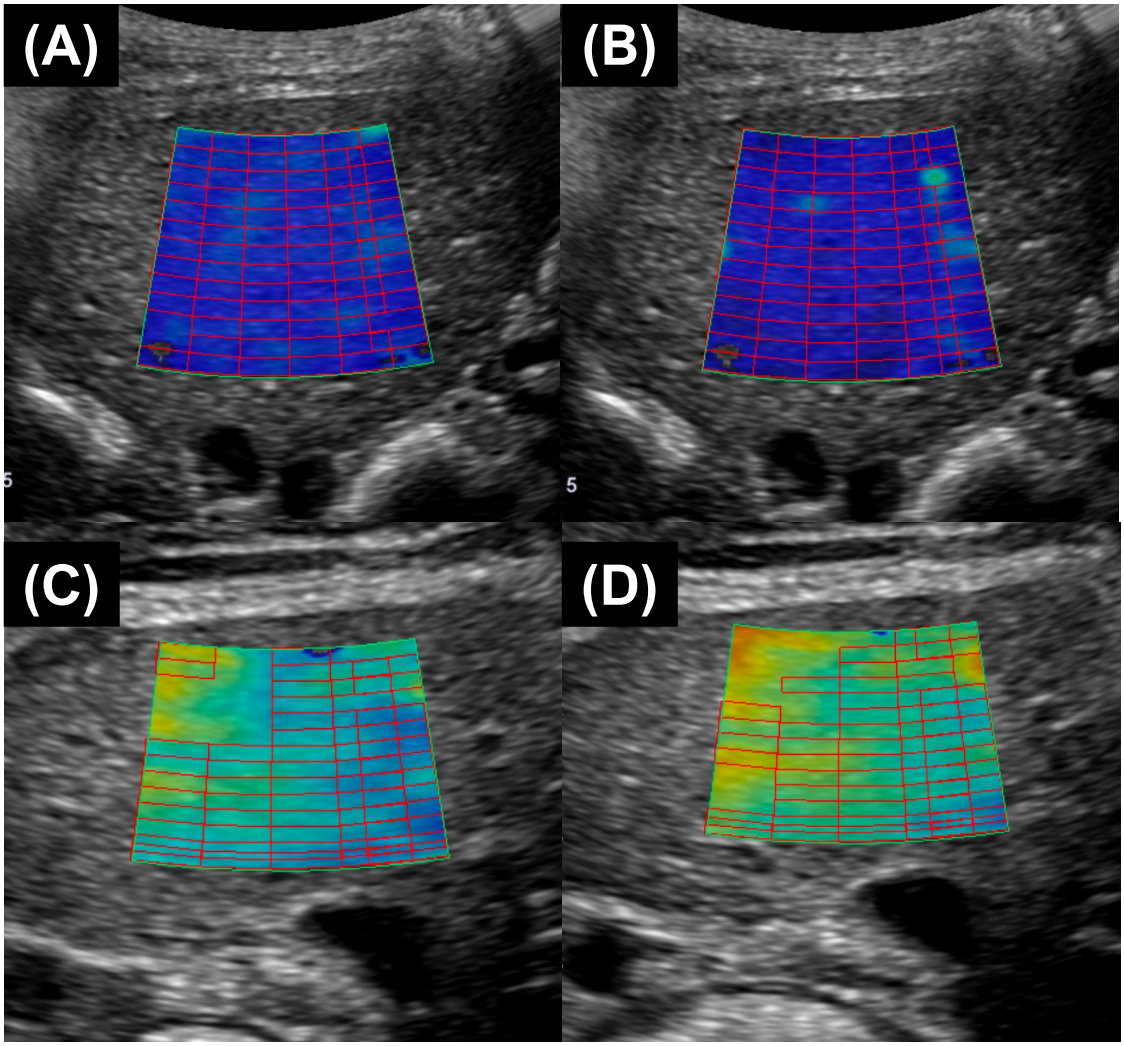

In many dogs in the non-RHF group, the color maps of SWS (A) and DS (B) were predominantly represented in dark blue. In contrast, in the RHF group, the color maps of both SWS (C) and DS (D) showed colors ranging from light blue to green and orange, indicating increased values.

Table 7. Correlation between SWS, DS, and each variable

	SWS		DS	
	P	r	*P*	r
Age	0.38		0.40	
Body weight	0.99		0.30	
ALT	0.18		0.27	
ALP	0.13		0.25	
T-Bill	0.46		0.35	
LA/Ao	0.70		0.91	
LVOT-VTI	<0.001	-0.40	<0.001	-0.38
TRV	<0.001	0.57	<0.001	0.58
RAA index	<0.001	0.69	<0.001	0.67
CVC SD/LD	<0.001	0.47	<0.001	0.56
SWS	-		<0.001	0.83

ALP: alkaline phosphatase; ALT: alanine aminotransferase; CVC SD/LD: ratio of short diameter and long diameter of caudal vena cava; DS: dispersion slope; LA/Ao: left atrial to aortic root ratio; LVOT-VTI: velocity time integral of left ventricular outflow tract; RAA index: right atrial area index; SWS: shear wave speed; T-Bill: total bilirubin; TRV: tricuspid regurgitant velocity

Table 8. AUCs and optimal diagnostic cutoffs for distinguishing dogs with and without RHF.

Variable	Cutoff	AUC [95% CI]	Sensitivity	Specificity	AIC
DS	14.2	0.977 [0.95-1.00]	0.962	0.918	36.6
SWS	1.51	0.945 [0.92-1.00]	0.846	0.945	41.8
CVC SD/LD	0.56	0.880 [0.81-0.95]	0.923	0.795	73.2
RAA index	14.0	0.870 [0.78-0.96]	0.739	0.903	68.7
LVOT-VTI	6.76	0.852 [0.76-0.94]	0.808	0.890	75.4
TRV	3.49	0.840 [0.74-0.94]	0.909	0.762	67.5

CVC SD/LD: ratio of short diameter and long diameter of caudal vena cava; DS: dispersion slope; LVOT-VTI: velocity time integral of left ventricular outflow tract; RAA index: right atrial area index; SWS: shear wave speed; TRV: tricuspid regurgitant velocity

Table 9. Stepwise multiple regression analysis of factors associated with SWS and DS

	SWS			DS	
	P	BIC		*P*	BIC
RAA index	<0.0001	64.6	CVC SD/LD	<0.0001	293.1
LVOT-VTI	0.0168	62.6	RAA index	0.0009	285.5
CVC SD/LD	0.0350	61.8	LVOT-VTI	0.1670	287.5
TRV	0.632	65.6	ALP	0.335	290.6
ALP	0.676	69.5	TRV	0.661	294.5
ALT	0.739	73.4	ALT	0.911	298.5

ALP: alkaline phosphatase; ALT: alanine aminotransferase; CVC SD/LD: ratio of short diameter and long diameter of caudal vena cava; DS: dispersion slope; LVOT-VTI: velocity time integral of left ventricular outflow tract; RAA index: right atrial area index; SWS: shear wave speed; TRV: tricuspid regurgitant velocity

4. Discussion

In In this study, the author evaluated the utility of 2D-SWE for assessing hepatic congestion in dogs with heart disease and found that both SWS and DS were significantly higher in dogs with RHF. These findings suggest that 2D-SWE, particularly DS, may serve as a useful noninvasive indicator for evaluating hepatic congestion associated with RHF.

SWS measurements in dogs with cardiac disease

SWS reflects both tissue viscosity and elasticity and is widely used in human medicine as an indicator of fibrosis in the diagnosis of liver diseases such as chronic hepatitis and cirrhosis[26-30, 69]. Similarly, studies in dogs have shown that SWS can detect liver fibrosis associated with primary hepatic disease[31]. Its usefulness in human patients with cardiac disease have also been investigated, with reports indicating that SWS increases with disease severity and correlates with echocardiographic parameters such as cardiac output, left ventricular volume, and right atrial size[39-42]. However, no previous reports have specifically evaluated SWS in veterinary patients with heart disease.

In the present study, 2D-SWE was performed in dogs with structural heart disease, and liver SWS was measured. Compared to the non-RHF group, the RHF group had significantly higher SWS values, which demonstrated high diagnostic accuracy for identifying RHF. Moderate correlations were observed between SWS and RAA index, CVC SD/LD, and LVOT-VTI.

Additionally, SWS was significantly associated with RAA index and CVC SD/LD, suggesting that increased SWS in dogs with heart disease reflects hepatic congestion associated with elevated right atrial volume and CVP. In addition, a significant association with LVOT-VTI may indicate that SWS may also be influenced by other factors, including liver fibrosis secondary to reduced cardiac output.

DS measurements in dogs with cardiac disease

Unlike SWS, DS specifically reflects tissue viscosity without being influenced by elasticity and is therefore considered particularly useful for evaluating viscous changes such as congestion and inflammation. In human studies, DS has been reported to correlate significantly with the severity of heart failure and echocardiographic indices[39, 41], and, importantly, to be independently associated with major cardiac events including cardiac death and the development of heart failure[40]. These findings suggest its potential as a novel marker for severity in cardiac disease.

In the present study, ROC analysis revealed that DS achieved the highest AUC (0.977 [0.95–1.00]), clearly indicating superior diagnostic ability for RHF compared with SWS and conventional echocardiographic parameters. In addition, DS was moderately associated with RAA index, CVC SD/LD, and LVOT-VTI, which were comparable to those observed for SWS. However, in stepwise multiple regression analysis, DS remained strongly associated with the CVC SD/LD and the RAA index, while no significant relationship was observed with LVOT-VTI.

These findings suggest that DS is a viscosity-specific parameter that is less influenced by alterations in cardiac output related to hypoperfusion or fibrosis, thereby more selectively reflecting hepatic congestion. Taken together, our results indicate that DS is superior to SWS in discriminating RHF and assessing hepatic congestion and may represent a useful noninvasive marker for the early detection and severity evaluation of hepatic congestion in dogs with cardiac disease.

Comparison with Conventional Ultrasonographic Parameters

In this study, the author simultaneously measured CVC SD/LD and the RAA index, which have been reported as useful indices for evaluating systemic congestion and right heart volume load, and compared their diagnostic performance with that of SWS and DS obtained by 2D-SWE. Previous studies demonstrated that in canine right heart disease, CVC SD/LD provides high diagnostic accuracy for RHF, with an AUC of 0.925 (95% CI: 0.865–0.986) at a cutoff of 0.665[23]. Similarly, indices of right atrial area[66, 70], such as the RAA index has been shown to strongly correlate with prognosis in canine PH, with an AUC of 0.97 (95% CI: 0.92–1.01) for the diagnosis of RHF when using a cutoff of 12.3 cm^2/m^2.

In the present study, both CVC SD/LD and the RAA index were significantly higher in dogs with RHF, confirming their role as indices reflecting right-sided cardiac overload. However, their diagnostic performance was lower than previously reported (CVC SD/LD: AUC 0.88; RAA index: AUC 0.87) and also inferior to SWS and DS. This discrepancy may be attributed to heterogeneity in the study population. Previous studies primarily investigated relatively homogeneous cohorts, such as dogs with isolated right heart disease or PH, whereas the present study included various underlying cardiac diseases (MMVD, congenital heart disease, cardiomyopathy, PH), resulting in a wide spectrum of right heart volume and congestion. Morphological indices such as the RAA index and CVC SD/LD may be particularly susceptible to inter-disease variability. For example, the RAA index is influenced by left atrial enlargement, leading to potential underestimation of right atrial size in dogs with left-sided heart disease such as MMVD. Furthermore, the RAA index primarily reflects chronic right atrial remodeling and may underestimate acute congestion. Similarly, CVC SD/LD reflects structural changes associated with elevated CVP but may fail to capture transient or acute elevations, particularly in chronic disease stages.

In contrast, SWS and DS obtained by 2D-SWE demonstrated superior diagnostic accuracy for RHF across a broad range of underlying diseases and disease stages. These findings suggest that SWS and DS may serve as more reliable and useful indices of systemic congestion in dogs with diverse cardiac conditions.

Correlation of SWS with Liver Fibrosis

Decreased cardiac output is an important pathophysiological component of heart failure, along with systemic congestion, and is thought to influence alterations in hepatic viscoelasticity. A reduction in cardiac output accompanied by decreased hepatic blood flow is associated with hypoxic hepatitis or cardiogenic liver injury, which is characterized by centrilobular necrosis and sinusoidal dysfunction, and has been implicated in the development of liver fibrosis [3-5,9-11]. Moreover, chronic hepatic congestion is known to promote hepatocellular necrosis and the formation of fibrotic bridges between central veins, ultimately progressing to hepatic fibrosis or cirrhosis[4,5]. Whereas hepatic congestion is considered a reversible condition, hepatic fibrosis is

irreversible, and the presence of fibrosis has been suggested as a prognostic factor in patients with heart disease[71-74]. Therefore, evaluating hepatic fibrosis in the context of heart disease is clinically important.

The LVOT-VTI used in this study is an established indicator that shows strong correlation with cardiac output measured by pulmonary artery catheterization[75,76]. In our study, LVOT-VTI was significantly lower in the RHF group, indicating that cardiac output was reduced in dogs with RHF. Furthermore, we found a negative correlation (r = –0.40) between SWS and LVOT-VTI, suggesting that reduced cardiac output may contribute to increased liver viscoelasticity in dogs with heart disease. Although multiple regression analysis showed no significant association between LVOT-VTI and DS (P = 0.1670), it revealed a significant association between LVOT-VTI and SWS (P = 0.0168). These findings imply that the elevation of SWS in dogs with heart disease may reflect not only hepatic congestion but also increased elasticity, indicative of fibrosis, secondary to reduced cardiac output.

Clinical Implications

The findings of this study indicate that 2D-SWE, particularly DS, represents a promising noninvasive modality for detecting hepatic congestion in dogs with heart disease. Because DS is relatively resistant to elastic changes such as fibrosis, it may serve as a sensitive and specific indicator of hepatic congestion secondary to RHF, with potential utility for early diagnosis and severity assessment. In addition, SWS may reflect not only hepatic congestion but also the progression of fibrosis due to hypoperfusion, thereby providing insight into the complex hepatic pathophysiology associated with heart disease. These indicators may also facilitate treatment monitoring, as improvements in right ventricular pressure overload and cardiac output achieved through therapies such as diuretics or cardiac glycosides may be quantitatively reflected as improvements in hepatic viscoelasticity. Furthermore, given their feasibility for repeated, noninvasive measurements, these modalities may be particularly useful for the serial evaluation of disease status, which has been challenging with conventional invasive approaches such as catheterization. Further investigations with larger cohorts are warranted to establish their clinical applicability.

Limitations

This study has several limitations. First, it was conducted at a single institution, raising the possibility of selection bias. Notably, the distribution of underlying heart diseases differed between the RHF and non-RHF groups, which may have influenced the results. Second, although cases with overt liver abnormalities or a history of liver disease were excluded, the absence of histological confirmation means that occult liver disease could not be completely ruled out, potentially affecting the findings. Third, direct measurement of CVP or RAP via catheterization was not performed, limiting the accuracy of congestion assessment. Finally, as this was a cross-sectional study with assessments performed at a single time point, longitudinal studies are required to clarify the temporal changes in 2D-SWE measurements with RHF progression or treatment.

5. Summary

In this chapter, the author investigated the utility of 2D-SWE for evaluating hepatic congestion in dogs with structural heart disease. Both SWS and DS were significantly elevated in dogs with RHF, indicating the presence of hepatic congestion or fibrosis.

SWS reflects combined tissue elasticity and viscosity, and in this study, its elevation was associated not only with congestion but also cardiac output. In contrast, DS specifically reflects tissue viscosity and demonstrated superior diagnostic accuracy for identifying RHF. DS showed strong associations with right atrial enlargement and CVC indices, suggesting that it reliably reflects hepatic congestion independent of cardiac output alterations.

Compared with conventional ultrasonographic parameters such as CVC SD/LD and right atrial area, SWS and DS showed higher diagnostic performance across a broad range of underlying cardiac diseases, supporting their value as noninvasive, quantitative biomarkers of liver involvement in heart disease.

In particular, DS appeared less influenced by fibrosis or cardiac output, supporting its value as a sensitive and specific indicator of hepatic congestion, with potential applications for early detection, severity assessment and potentially monitoring treatment response in dogs with heart disease.

General Conclusion

This study demonstrated the clinical value of 2D-SWE for noninvasively assessing hepatic changes associated with both induced congestion and naturally occurring cardiac disease in dogs.

In Chapter 1, which evaluated hepatic congestion induced by volume loading (blood transfusion), both SWS and DS increased significantly following volume loading, indicating that these 2D-SWE parameters reflect hepatic congestion induced by acute elevations in venous pressure. This change is thought to reflect elevated hepatic viscosity caused by passive hepatic congestion secondary to volume overload. Additionally, an important distinction emerged in their correlations with ultrasonographic congestion indices. DS showed a strong correlation with CVC SD/LD, a validated marker of systemic venous congestion, whereas the correlation between SWS and CVC SD/LD was only moderate. This suggests that DS is more sensitive than SWS to hemodynamic changes associated with congestion and may better capture viscosity-related alterations that occur in the early phase of hepatic venous hypertension.

In Chapter 2, which involved dogs with naturally occurring heart disease, both SWS and DS were significantly increased, indicating hepatic alterations secondary to cardiac dysfunction. Compared with Chapter 1, the correlations between SWS or DS and CVC SD/LD were weaker. In addition to venous congestion, other factors that increase hepatic viscoelasticity—such as hypoxic hepatitis associated with reduced cardiac output and fibrosis resulting from long-standing congestion—may also contribute to elevated SWS and DS in clinical patients. Supporting this interpretation, DS showed superior performance to SWS for detecting hepatic congestion, consistent with the findings of Chapter 1. Although histopathological confirmation was not available in this study, the collective findings across both chapters support a unified interpretation: DS is better suited for detecting hepatic congestion, whereas SWS may reflect more complex hepatic alterations associated with chronic cardiac disease,

including hypoxia-related injury, fibrosis, and other structural changes, suggesting that SWS captures cumulative hepatic remodeling beyond congestion alone.

Overall, this study highlights the utility of 2D-SWE—integrating the complementary strengths of SWS and DS—as a robust, quantitative, and noninvasive tool for evaluating hepatic pathophysiology in dogs with heart disease. This modality may offer significant advantages for early detection, distinguishing congestion from fibrosis, and monitoring therapeutic responses. Future studies incorporating histopathological validation in cardiac patients will further refine the diagnostic and prognostic applications of SWS and DS in veterinary cardiology.

Acknowledgement

This PhD study is not something I could have accomplished alone. I would like to express my sincere gratitude to all those who have supported and encouraged me throughout this journey.

First and foremost, I am deeply grateful to my supervisor, Dr. Mitsuyoshi Takiguchi, for his unwavering encouragement, insightful guidance, and continuous support during the entire course of this thesis.

I am also thankful to Drs. Takashi Kimura, Masahiro Yamasaki, Nozomu Yokoyama for generously providing valuable advice and constructive comments, which have significantly improved this dissertation.

My heartfelt appreciation goes to my mentor, Dr. Kensuke Nakamura, for his thoughtful critiques of my research, manuscripts, presentations, and this dissertation. Their mentorship has been indispensable, and this work would not have reached its current level of refinement without their dedicated support.

I further extend my gratitude to Drs. Noboru Sasaki, Keitaro Morishita, Sei Kawamoto, Masahiro Tamura (Rakuno Gakuen University), Mei Sugawara-Suda, Yumiko Kagawa (North Lab), Kazuyoshi Sasaoka for their continual guidance and assistance.

My appreciation also goes to my colleagues—Drs. Yuki Kawakami, Kei Sato, and all members of the Laboratory of Veterinary Internal Medicine—for their invaluable advice, collaboration, and friendship. I am equally grateful to all staff members of the Hokkaido University Veterinary Teaching Hospital for their support throughout my studies.

Finally, my deepest gratitude goes to my family and friends for their constant encouragement, understanding, and unwavering support.

References

1. Fortea JI, Puente Á, Cuadrado A, Huelin P, Pellón R, González Sánchez FJ, Mayorga M, Cagigal ML, García Carrera I, Cobreros M, Crespo J, Fábrega E. Congestive Hepatopathy. Int J Mol Sci. 2020 Dec 10;21(24):9420.
2. Lemmer A, VanWagner L, Ganger D. Congestive hepatopathy: Differentiating congestion from fibrosis. Clin Liver Dis (Hoboken). 2018 Jan 2;10(6):139-143.
3. Kavoliuniene A, Vaitiekiene A, Cesnaite G. Congestive hepatopathy and hypoxic hepatitis in heart failure: a cardiologist's point of view. Int J Cardiol. 2013 Jul 1;166(3):554-8.
4. Shah SC, Sass DA. “Cardiac Hepatopathy”: A Review of Liver Dysfunction in Heart Failure. *Liver Res - Open J.* 2015; 1:1–10.
5. Møller S, Bernardi M. Interactions of the heart and the liver. Eur Heart J. 2013 Sep;34(36):2804-11.
6. Dai DF, Swanson PE, Krieger EV, Liou IW, Carithers RL, Yeh MM. Congestive hepatic fibrosis score: a novel histologic assessment of clinical severity. Mod Pathol. 2014 Dec;27(12):1552-8.
7. Sugawara Y, Yoshihisa A, Ishibashi S, Matsuda M, Yamadera Y, Ohara H, Ichijo Y, Watanabe K, Hotsuki Y, Anzai F, Sato Y, Kimishima Y, Yokokawa T, Misaka T, Yamada S, Sato T, Kaneshiro T, Oikawa M, Kobayashi A, Takeishi Y. Liver Congestion Assessed by Hepatic Vein Waveforms in Patients With Heart Failure. CJC Open. 2021 Feb 7;3(6):778-786.
8. Ohara H, Yoshihisa A, Ishibashi S, Matsuda M, Yamadera Y, Sugawara Y, Ichijo Y, Sato Y, Misaka T, Sato T, Oikawa M, Kobayashi A, Takeishi Y. Hepatic Venous Stasis Index Reflects Hepatic Congestion and Predicts Adverse Outcomes in Patients With Heart Failure. J Am Heart Assoc. 2023 Jun 20;12(12):e029857.
9. Samsky MD, Patel CB, DeWald TA, Smith AD, Felker GM, Rogers JG, Hernandez AF. Cardiohepatic interactions in heart failure: an overview and clinical implications. J Am Coll Cardiol. 2013 Jun 18;61(24):2397-2405.
10. Zhan L, Huang C, Meng XM, Song Y, Wu XQ, Yang Y, Li J. Hypoxia-inducible factor-1alpha in hepatic fibrosis: A promising therapeutic target. Biochimie. 2015 Jan; 108:1-7.
11. Cai J, Hu M, Chen Z, Ling Z. The roles and mechanisms of hypoxia in liver fibrosis. J Transl Med. 2021 May 1;19(1):186.
12. Mele D, Pestelli G, Molin DD, Smarrazzo V, Luisi GA, Trevisan F, Fiorencis A,

Flamigni F, Ferrari R. Right Atrial Pressure Is Associated with Outcomes in Patients with Heart Failure and Indeterminate Left Ventricular Filling Pressure. J Am Soc Echocardiogr. 2020 Nov;33(11):1345-1356.

13. Chen Y, Shlofmitz E, Khalid N, Bernardo NL, Ben-Dor I, Weintraub WS, Waksman R. Right Heart Catheterization-Related Complications: A Review of the Literature and Best Practices. Cardiol Rev. 2020 Jan/Feb;28(1):36-41.
14. Borow M, Crowley JG. Evaluation of central venous catheter thrombogenicity. Acta Anaesthesiol Scand Suppl. 1985; 81:59-64.
15. Perondi F, Petrescu VF, Fratini F, Brovida C, Porciello F, Ceccherini G, Lippi I. Bacterial colonization of non-permanent central venous catheters in hemodialysis dogs. Heliyon. 2020 Jan 29;6(1): e03224.
16. Reminga CL, Silverstein DC, Drobatz KJ, Clarke DL. Evaluation of the placement and maintenance of central venous jugular catheters in critically ill dogs and cats. J Vet Emerg Crit Care (San Antonio). 2018 May;28(3):232-243.
17. Sharma S, Khalili K, Nguyen GC. Non-invasive diagnosis of advanced fibrosis and cirrhosis. World J Gastroenterol. 2014 Dec 7;20(45):16820-30.
18. Seeff LB, Everson GT, Morgan TR, Curto TM, Lee WM, Ghany MG, Shiffman ML, Fontana RJ, Di Bisceglie AM, Bonkovsky HL, Dienstag JL; HALT–C Trial Group. Complication rate of percutaneous liver biopsies among persons with advanced chronic liver disease in the HALT-C trial. Clin Gastroenterol Hepatol. 2010 Oct;8(10):877-83.
19. Dhall D, Kim SA, Mc Phaul C, Kransdorf EP, Kobashigawa JA, Sundaram V, Mirocha J, Guindi M. Heterogeneity of Fibrosis in Liver Biopsies of Patients With Heart Failure Undergoing Heart Transplant Evaluation. Am J Surg Pathol. 2018 Dec;42(12):1617-1624.
20. Nelson NC, Drost WT, Lerche P, Bonagura JD. Noninvasive estimation of central venous pressure in anesthetized dogs by measurement of hepatic venous blood flow velocity and abdominal venous diameter. Vet Radiol Ultrasound. 2010 May-Jun;51(3):313-23.
21. Ciozda W, Kedan I, Kehl DW, Zimmer R, Khandwalla R, Kimchi A. The efficacy of sonographic measurement of inferior vena cava diameter as an estimate of central venous pressure. Cardiovasc Ultrasound. 2016 Aug 20;14(1):33.
22. Beigel R, Cercek B, Luo H, Siegel RJ. Noninvasive evaluation of right atrial pressure. J Am Soc Echocardiogr. 2013 Sep;26(9):1033-42.

23. Fujioka T, Nakamura K, Minamoto T, Tsuzuki N, Yamaguchi J, Hidaka Y. Ultrasonographic evaluation of the caudal vena cava in dogs with right-sided heart disease. J Vet Cardiol. 2021 Apr; 34:80-92.
24. Ma Q, Shi X, Ji J, Chen L, Tian Y, Hao J, Li B. The diagnostic accuracy of inferior vena cava respiratory variation in predicting volume responsiveness in patients under different breathing status following abdominal surgery. BMC Anesthesiol. 2022 Mar 8;22(1):63.
25. Darnis E, Merveille AC, Desquilbet L, Boysen S, Gommeren K. Interobserver agreement between non-cardiologist veterinarians and a cardiologist after a 6-hour training course for echographic evaluation of basic echocardiographic parameters and caudal vena cava diameter in 15 healthy Beagles. J Vet Emerg Crit Care (San Antonio). 2019 Sep;29(5):495-504.
26. Osaki A, Kubota T, Suda T, Igarashi M, Nagasaki K, Tsuchiya A, Yano M, Tamura Y, Takamura M, Kawai H, Yamagiwa S, Kikuchi T, Nomoto M, Aoyagi Y. Shear wave velocity is a useful marker for managing nonalcoholic steatohepatitis. World J Gastroenterol. 2010 Jun 21;16(23):2918-25.
27. Xiao G, Zhu S, Xiao X, Yan L, Yang J, Wu G. Comparison of laboratory tests, ultrasound, or magnetic resonance elastography to detect fibrosis in patients with nonalcoholic fatty liver disease: A meta-analysis. Hepatology. 2017 Nov;66(5):1486-1501.
28. Ferraioli G, Tinelli C, Lissandrin R, Zicchetti M, Dal Bello B, Filice G, Filice C. Point shear wave elastography method for assessing liver stiffness. World J Gastroenterol. 2014 Apr 28;20(16):4787-96.
29. Zhuang Y, Ding H, Zhang Y, Sun H, Xu C, Wang W. Two-dimensional Shear-Wave Elastography Performance in the Noninvasive Evaluation of Liver Fibrosis in Patients with Chronic Hepatitis B: Comparison with Serum Fibrosis Indexes. Radiology. 2017 Jun;283(3):873-882.
30. Frulio N, Trillaud H. Ultrasound elastography in liver. Diagn Interv Imaging. 2013 May;94(5):515-34.
31. Tamura M, Ohta H, Shimbo G, Osuga T, Sasaki N, Morishita K, Kagawa Y, Takiguchi M. Usefulness of noninvasive shear wave elastography for the assessment of hepatic fibrosis in dogs with hepatic disease. J Vet Intern Med. 2019 Sep;33(5):2067-2074.
32. Barry CT, Mills B, Hah Z, Mooney RA, Ryan CK, Rubens DJ, Parker KJ. Shear wave dispersion measures liver steatosis. Ultrasound Med Biol. 2012 Feb;38(2):175-82.

33. Barry CT, Hah Z, Partin A, Mooney RA, Chuang KH, Augustine A, Almudevar A, Cao W, Rubens DJ, Parker KJ. Mouse liver dispersion for the diagnosis of early-stage Fatty liver disease: a 70-sample study. Ultrasound Med Biol. 2014 Apr;40(4):704-13.
34. Sugimoto K, Moriyasu F, Oshiro H, Takeuchi H, Yoshimasu Y, Kasai Y, Furuichi Y, Itoi T. Viscoelasticity Measurement in Rat Livers Using Shear-Wave US Elastography. Ultrasound Med Biol. 2018 Sep;44(9):2018-2024.
35. Sugimoto K, Moriyasu F, Oshiro H, Takeuchi H, Yoshimasu Y, Kasai Y, Itoi T. Clinical utilization of shear wave dispersion imaging in diffuse liver disease. Ultrasonography. 2020 Jan;39(1):3-10.
36. Xie LT, Xu DX, Tian G, Zhong LY, Zhao QY, Ke QH, Jiang TA. Value of Two-Dimensional Shear Wave Elastography for Assessing Acute Liver Congestion in a Bama Mini-Pig Model. Dig Dis Sci. 2018 Jul;63(7):1851-1859.
37. Millonig G, Friedrich S, Adolf S, Fonouni H, Golriz M, Mehrabi A, Stiefel P, Pöschl G, Büchler MW, Seitz HK, Mueller S. Liver stiffness is directly influenced by central venous pressure. J Hepatol. 2010 Feb;52(2):206-10.
38. Tamura M, Ohta H, Osuga T, Takiguchi M. Effectiveness of 2-dimensional shear wave elastography for noninvasive and reliable estimation of right atrial pressure in dogs with induced volume overload. J Vet Intern Med. 2023 May-Jun;37(3):866-874.
39. Yoshihisa A, Ishibashi S, Matsuda M, Yamadera Y, Ichijo Y, Sato Y, Yokokawa T, Misaka T, Oikawa M, Kobayashi A, Yamaki T, Kunii H, Takeishi Y. Clinical Implications of Hepatic Hemodynamic Evaluation by Abdominal Ultrasonographic Imaging in Patients with Heart Failure. J Am Heart Assoc. 2020 Aug 4;9(15)
40. Ohara H, Yoshihisa A, Ishibashi S, Matsuda M, Yamadera Y, Sugawara Y, Ichijo Y, Hotsuki Y, Watanabe K, Anzai F, Sato Y, Kimishima Y, Yokokawa T, Misaka T, Sato T, Oikawa M, Kobayashi A, Takeishi Y. Shear Wave Dispersion Predicts Liver Fibrosis and Adverse Outcomes in Patients with Heart Failure. J Clin Med. 2020 Dec 6;9(12):3953.
41. Nakayama R, Takaya Y, Nakamura K, Toh N, Ito H. Efficacy of shear wave elastography for assessment of liver function in patients with heart failure. ESC Heart Fail. 2021 Jun;8(3):1751-1758.
42. Urabe C, Takaya Y, Nakayama R, Nakamura K, Ito H. Shear Wave Dispersion Slope of the Liver Can Predict Adverse Outcomes in Patients with Pulmonary Hypertension. Int Heart J. 2023 Mar 31;64(2):230-236.
43. Ferraioli G, Wong VW, Castera L, Berzigotti A, Sporea I, Dietrich CF, Choi BI,

Wilson SR, Kudo M, Barr RG. Liver Ultrasound Elastography: An Update to the World Federation for Ultrasound in Medicine and Biology Guidelines and Recommendations. Ultrasound Med Biol. 2018 Dec;44(12):2419-2440.

44. Jung JW, Je H, Lee SK, Jang Y, Choi J. Two-Dimensional Shear Wave Elastography of Normal Soft Tissue Organs in Adult Beagle Dogs; Interobserver Agreement and Sources of Variability. Front Bioeng Biotechnol. 2020 Aug 19; 8:979.
45. Rudski LG, Lai WW, Afilalo J, Hua L, Handschumacher MD, Chandrasekaran K, Solomon SD, Louie EK, Schiller NB. Guidelines for the echocardiographic assessment of the right heart in adults: a report from the American Society of Echocardiography endorsed by the European Association of Echocardiography, a registered branch of the European Society of Cardiology, and the Canadian Society of Echocardiography. J Am Soc Echocardiogr. 2010 Jul;23(7):685-713; quiz 786-8.
46. Chen L, Hsiao A, Langhan M, Riera A, Santucci KA. Use of bedside ultrasound to assess degree of dehydration in children with gastroenteritis. Acad Emerg Med. 2010 Oct;17(10):1042-7.
47. Babaie S, Behzad A, Mohammadpour M, Reisi M. A Comparison between the Bedside Sonographic Measurements of the Inferior Vena Cava Indices and the Central Venous Pressure While Assessing the Decreased Intravascular Volume in Children. Adv Biomed Res. 2018 Jun 25; 7:97.
48. Seo Y, Iida N, Yamamoto M, Machino-Ohtsuka T, Ishizu T, Aonuma K. Estimation of Central Venous Pressure Using the Ratio of Short to Long Diameter from Cross-Sectional Images of the Inferior Vena Cava. J Am Soc Echocardiogr. 2017 May;30(5):461-467.
49. Sato Y, Kawataki M, Hirakawa A, Toyoshima K, Kato T, Itani Y, Hayakawa M. The diameter of the inferior vena cava provides a noninvasive way of calculating central venous pressure in neonates. Acta Paediatr. 2013 Jun;102(6):e241-6.
50. Arena U, Vizzutti F, Corti G, Ambu S, Stasi C, Bresci S, Moscarella S, Boddi V, Petrarca A, Laffi G, Marra F, Pinzani M. Acute viral hepatitis increases liver stiffness values measured by transient elastography. Hepatology. 2008 Feb;47(2):380-4.
51. Yoshioka K, Kawabe N, Hashimoto S. Transient elastography: Applications and limitations. Hepatol Res. 2008;38(11):1063-8.
52. Millonig G, Reimann FM, Friedrich S, Fonouni H, Mehrabi A, Büchler MW, Seitz HK, Mueller S. Extrahepatic cholestasis increases liver stiffness (FibroScan) irrespective of fibrosis. Hepatology. 2008 Nov;48(5):1718-23.

53. Attia D, Pischke S, Negm AA, Rifai K, Manns MP, Gebel MJ, Lankisch TO, Potthoff A. Changes in liver stiffness using acoustic radiation force impulse imaging in patients with obstructive cholestasis and cholangitis. Dig Liver Dis. 2014 Jul;46(7):625-31.
54. Tamura M, Ohta H, Osuga T, Sasaki N, Morishita K, Takiguchi M. Extrahepatic biliary obstruction can interfere with hepatic fibrosis prediction using two-dimensional shear wave elastography in dogs. Vet Radiol Ultrasound. 2021 Jul;62(4):483-489.
55. Kong W, Tang Y, Liu L, Zhang G, Liu Y, Liu J. Stratifying Non-alcoholic Steatohepatitis With the Non-invasive Ultrasound Markers Shear Wave Dispersion Slope and Shear Wave Velocity: An Animal Study. Ultrasound Med Biol. 2022 Dec;48(12):2442-2448.
56. Song SJ, Kim YR, Lee YH, Cho EY. Potential role of two-dimensional shear wave elastography, including liver stiffness measurement and dispersion slope, for management of chronic hepatitis B. Ultrasonography. 2024 Sep;43(5):384-392.
57. Yazdani L, Rafati I, Gesnik M, Nicolet F, Chayer B, Gilbert G, Volniansky A, Olivié D, Giard JM, Sebastiani G, Nguyen BN, Tang A, Cloutier G. Ultrasound Shear Wave Attenuation Imaging for Grading Liver Steatosis in Volunteers and Patients With Non-alcoholic Fatty Liver Disease: A Pilot Study. Ultrasound Med Biol. 2023 Oct;49(10):2264-2272.
58. Delgado-Valero B, Cachofeiro V, Martínez-Martínez E. Fibrosis, the Bad Actor in Cardiorenal Syndromes: Mechanisms Involved. Cells. 2021 Jul 19;10(7):1824.
59. Xu X, Zhang B, Wang Y, Shi S, Lv J, Fu Z, Gao X, Li Y, Wu H, Song Q. Renal fibrosis in type 2 cardiorenal syndrome: An update on mechanisms and therapeutic opportunities. Biomed Pharmacother. 2023 Aug; 164:114901.
60. Egbe AC, Reddy YNV, Khan AR, Al-Otaibi M, Akintoye E, Obokata M, Borlaug BA. Venous congestion and pulmonary vascular function in Fontan circulation: Implications for prognosis and treatment. Int J Cardiol. 2018 Nov 15; 271:312-316.
61. Guinot PG, Longrois D, Andrei S, Nguyen M, Bouhemad B; CodOrea study group. Exploring congestion endotypes and their distinct clinical outcomes among ICU patients: A post-hoc analysis. Anaesth Crit Care Pain Med. 2024 Jun;43(3):101370.
62. Yogeswaran A, Richter MJ, Husain-Syed F, Rako Z, Sommer N, Grimminger F, Seeger W, Ghofrani HA, Gall H, Tello K. Estimated plasma volume status: association with congestion, cardiorenal syndrome and prognosis in precapillary pulmonary hypertension. Front Cardiovasc Med. 2023 May 10; 10:1161041.
63. Reinero C, Visser LC, Kellihan HB, Masseau I, Rozanski E, Clercx C, Williams K,

Abbott J, Borgarelli M, Scansen BA. ACVIM consensus statement guidelines for the diagnosis, classification, treatment, and monitoring of pulmonary hypertension in dogs. J Vet Intern Med. 2020 Mar;34(2):549-573.

64. Rishniw M, Erb HN. Evaluation of four 2-dimensionalechocardiographic methods of assessing left atrial size in dogs. JVet Intern Med 2000;14:429–435.
65. Dickson D, Caivano D, Patteson M, Rishniw M. The timesthey are a-changin': Two-dimensional aortic valve measurementsdiffer throughout diastole. J Vet Cardiol 2016;18:15
66. Vezzosi T, Domenech O, Iacona M, Marchesotti F, Zini E, Venco L, Tognetti R. Echocardiographic Evaluation of the Right Atrial Area Index in Dogs with Pulmonary Hypertension. J Vet Intern Med. 2018 Jan;32(1):42-47.
67. S Swets JA. Measuring the accuracy of diagnostic systems. Science. 1988 Jun 3;240(4857):1285-93.
68. Fluss R, Faraggi D, Reiser B. Estimation of the Youden Index and its associated cutoff point. Biom J. 2005 Aug;47(4):458-72.
69. Ferraioli G, Parekh P, Levitov AB, Filice C. Shear wave elastography for evaluation of liver fibrosis. J Ultrasound Med. 2014 Feb;33(2):197-203.
70. Visser LC, Wood JE, Johnson LR. Survival characteristics and prognostic importance of echocardiographic measurements of right heart size and function in dogs with pulmonary hypertension. J Vet Intern Med. 2020 Jul;34(4):1379-1388.
71. Myhre PL, Grupper A, Mebazaa A, Davison B, Edwards C, Takagi K, Adamo M, Arrigo M, Barros M, Biegus J, Celutkiene J, Čerlinskaitė-Bajorė K, Chioncel O, Cohen-Solal A, Damasceno A, Deniau B, Diaz R, Filippatos G, Gayat E, Kimmoun A, Ter Maaten JM, Metra M, Novosadova M, Pagnesi M, Pang PS, Ponikowski P, Saidu H, Sliwa K, Tomasoni D, Voors A, Cotter G, Lam CSP. Changes in Liver Function Tests, Congestion, and Prognosis After Acute Heart Failure: The STRONG-HF Trial. JACC Adv. 2025 Mar;4(3):101607.
72. Yoshihisa A, Sato Y, Yokokawa T, Sato T, Suzuki S, Oikawa M, Kobayashi A, Yamaki T, Kunii H, Nakazato K, Saitoh SI, Takeishi Y. Liver fibrosis score predicts mortality in heart failure patients with preserved ejection fraction. ESC Heart Fail. 2018 Apr;5(2):262-270.
73. Cao Y, Guo S, Dong Y, Liu C, Zhu W. Comparison of liver fibrosis scores for predicting mortality and morbidity in heart failure with preserved ejection fraction. ESC Heart Fail. 2023 Jun;10(3):1771-1780.
74. Varela-Cancelo A, Barge-Caballero E, Barge-Caballero G, Couto-Mallón D, Paniagua-Martín MJ, Antúnez-Ballesteros M, Enríquez-Vázquez D, Grille-Cancela

Z, Muñiz J, Vázquez-Rodríguez JM, Crespo-Leiro MG. Prognostic value of liver fibrosis scores in ambulatory patients with heart failure. Postgrad Med. 2025 Apr-May;137(3-4):274-286.

75. Aslan N, Yildizdas D, Horoz OO, Coban Y, Demir F, Erdem S, Sertdemir Y. Comparison of cardiac output and cardiac index values measured by critical care echocardiography with the values measured by pulse index continuous cardiac output (PiCCO) in the pediatric intensive care unit: a preliminary study. Ital J Pediatr. 2020 Apr 16;46(1):47.
76. Aligholizadeh E, Teeter W, Patel R, Hu P, Fatima S, Yang S, Ramani G, Safadi S, Olivieri P, Scalea T, Murthi S. A novel method of calculating stroke volume using point-of-care echocardiography. Cardiovasc Ultrasound. 2020 Aug 20;18(1):37.

Summary in Japanese（和文要旨）

Study on the assessment of hepatic congestion and fibrosis in dogs with cardiac disease using Shear Wave Elastography
（犬の心疾患における剪断波エラストグラフィを用いた肝うっ血および肝線維化の評価に関する研究）

心不全は、弁膜疾患、心筋症、肺高血圧症など多様な心疾患が進行し、代償機構が破綻することで生じる病態であり、肝機能障害を含む多臓器不全へとつながる臨床症候群である。心不全に伴う代表的な病態は「うっ血」と「低心拍出」であり、これらが全身の臓器障害の主因となる。うっ血性右心不全（RHF）では中心静脈圧（CVP）が上昇し、受動的な肝うっ血が生じる。これにより肝静脈や類洞の拡張、肝細胞の萎縮や壊死といった変化が起こり、うっ血が長期間続くことで肝線維化へと進展することが知られている。また、肝うっ血はヒトの心不全患者では重要な予後決定因子であると考えられているにもかかわらず、その重症度を正確かつ非侵襲的に評価する方法は十分に確立されていない。一方、心拍出量の低下は全身の動脈圧や組織灌流の低下を引き起こす。肝臓の灌流が不足すると、肝細胞の低酸素状態が進行し、小葉中心性壊死を主体としたびまん性肝障害が生じる。この病態は「低酸素性肝炎」や「低酸素性肝障害」などと呼ばれ、うっ血と同様に慢性的に持続することにより肝線維化の進展に関与すると考えられている。

このように、肝臓と心臓は病態生理学的に密接に関連しており、心疾患患者においては、早期のうちから心不全の管理だけでなく、肝うっ血および肝機能障害を適切に評価することが極めて重要である。うっ血の評価のゴールドスタンダードはカテーテルによる CVP や右心房圧（RAP）の直接的な測定であり、肝うっ血や肝線維化の評価には肝生検による病理組織学的な評価が必要となる。しかし、これらの検査は全身麻酔を必要とし、合併症を生じうる侵襲的な検査であることから臨床現場でのルーチンでの実施は困難である。以上の背景から、心疾患患者における肝うっ血や肝線維化などの肝臓の病態を非侵襲的かつ定量的に評価する検査法の確立が求められている。

二次元剪断波エラストグラフィ（2D-SWE）は、肝臓を含む臓器の硬さを非侵襲的に定量化できる超音波技術である。2D-SWE で得られる Shear wave speed（SWS）は、組織の粘性と弾性の両方を反映する粘弾性の指標である一方、Dispersion slope（DS）は、弾性には依存せず粘性のみを評価できる粘性の指標である。組織の弾性は主に線維化により上昇する一方で、粘性は炎症やうっ血

などにより上昇することが知られている。肝臓においてうっ血や炎症は可逆的な病態であるが、線維化はこれらが進行した末期的な病態であり、非可逆的な病理変化である。本研究では二つの章にわたり、心疾患犬における SWS および DS の病態評価における有用性を検討した。

第一章では、急性肝うっ血モデルとして輸血を実施した臨床例を用いて、SWS・DS が容量負荷に伴う肝うっ血によりどのように変化するかを検討した。その結果、SWS および DS はともには輸血後に有意に上昇し、肝うっ血に伴う肝硬度（粘弾性）の上昇を反映することが示された。特に DS はうっ血指標である後大静脈短径長径比（CVC SD/LD）と強い相関を示し、SWS と CVC SD/LD の相関は中等度にとどまった。これにより、うっ血に伴う粘性変化の評価には DS がより鋭敏であることが明らかとなった。

第二章では、自然発生の心疾患犬を対象に、心疾患における肝臓の SWS・DS の変化およびその臨床的有用性ならびに指標の変動をもたらす因子を評価した。うっ血の指標としては第一章と同様に CVC SD/LD を用い、右心系の指標として右心房面積を、心拍出量の指標として左室一回拍出量（LVOT-VTI）を測定した。症例を RHF 徴候の有無により、RHF 群と非 RHF に分けて比較したところ、SWS および DS は RHF 群において有意な上昇を示した。特に DS は RHF の識別能が既存の指標と比較して最も高かった（AUC 0.977）。また DS の上昇に CVC SD/LD や右心房面積は関連を示したが、心拍出量の指標である LVOT-VTI とは関連が認められなかった。第一章の結果と合わせると、心疾患の臨床例においても DS はうっ血を特異的に反映する粘性指標であることが示唆された。一方で、SWS の上昇には上記のうっ血や右心系に加えて、LVOT - VTI との関連も認めた。このことから、SWS の上昇はうっ血だけではなく低心拍出に伴う二次的な肝線維化などの弾性変化の病態も捉えることができる可能性が示された。

以上の結果から、SWS と DS を併用することで、心疾患の犬の肝臓に生じる線維化やうっ血といった異なる病態生理学的変化を補完的に評価できることが示された。特に DS が心疾患を有する犬における肝うっ血の検出において有望な非侵襲的ツールであることを示唆している。DS は線維化などの弾性変化の影響を受けにくい特性から、RHF に起因する肝うっ血の鋭敏かつ特異的な指標となり得ることが示唆され、早期診断および重症度評価への応用が期待される。また、SWS はうっ血だけでなく、低灌流による線維化の進行なども反映する可能性があり、心疾患に伴う複合的な肝臓の変化を把握する上で臨床的に有用となる可能性が示唆された。これらの指標は、心不全症例の治療効果のモニタリングにも応用可能であり、利尿薬や強心薬の心不全治療による右心系圧負荷の軽減や心拍出量の改善が、肝臓の粘弾性の改善として数値に反映される可

能性がある。また、繰り返し測定が可能であるため、従来のカテーテル検査等の侵襲的手法では困難であった病態の経時的評価にも有用であると考えられ臨床応用に向けたさらなる検討と症例蓄積が望まれる。

本研究は、2D-SWE が犬の心疾患に伴う肝臓病態を非侵襲的かつ定量的に評価する有力なツールであることを示した。特に DS は線維化や心拍出量の影響を受けにくく、肝うっ血の鋭敏かつ特異的な指標となり、うっ血の早期検出や重症度評価に有用となる可能性が示唆された。今後は、より大規模かつ縦断的な研究を通じて、心疾患犬に対する 2D-SWE の診断的・予後的有用性および治療反応性との関連についての検討が期待される。